VERIFICATION

# UDM CHAPTER 8: TIME-VARYING RELEASES

DATE: December 2023

Reference to part of this report which may lead to misinterpretation is not permissible.

| No. | Date | Reason for Issue | Prepared by | Verified by | Approved by |
|---|---|---|---|---|---|
| 1 | August 2014 | UDM AWD | Witlox | Harper | |
| | | Gravity shape correction | | | |
| 2 | May 2021 | Apply new template | | | |

Date: December 2023

**Prepared by: Digital Solutions at DNV**

## ABSTRACT

This report documents the verification of the new UDM time-varying dispersion model, which includes modelling of effects of along-wind-diffusion (AWD) and effects of along-wind gravity spreading.

First UDM AWD has been verified analytically for both steady-state and finite-duration passive dispersion (horizontal releases):

- Ermak's FDC (Finite Duration Correction) equations applicable for an unpressurised passive constant finite-duration ground-level release have been re-derived, including an analytical derivation of values for the maximum concentration over all times. Ermak assumes that the cloud moves with the effective speed $u_{eff,}$ which for a non-constant wind-speed profile is larger than the UDM cloud speed at cloud centroid height.
- Ermak's FDC and UDM AWD equations for concentrations have been compared for both time-varying and finite-duration releases, where it has been demonstrated that the UDM AWD formulation appears to be more realistic than the FDC formulation. Temporary adjustments to both formulations ion order to remove all differences have been applied to confirm close matching of results of both UDM AWD and UDM FDC formulations with analytical solutions obtained for both average cloud speed and concentration versus time at a given distance.

Secondly UDM AWD has been verified for the case of time-varying releases. This first includes verification against the time-varying HGSYSTEM 3.0 model HEGADAS-T for the case of dispersion from a pool. Secondly it includes a comparison between the new UDM AWD model and old UDM segment-model (no AWD effects) for the case of an elevated finite-duration release with rainout, and the case of an elevated time-varying multi-component toxic release from a long pipeline with rainout. Significantly reduced concentrations and doses are shown to be obtained for the new UDM AWD formulations.

Finally the along-wind gravity spreading correction (GSC) has been verified against analytical spreadsheet calculations. This first includes unpressurised steady-state and finite-duration releases from a ground-level area source corresponding to the Kit Fox releases. It has been verified that for the available experiments (URA continuous and URA puff) GSC does not significantly affect the validation, because the ambient velocities are not sufficiently low. Secondly GSC has been tested for elevated horizontal jet releases without and with rainout.

# Table of contents



# Table of figures



# List of tables

# 8 INTRODUCTION

This report documents the verification of the UDM dispersion model for the case of time-varying releases. In this report UDM AWD refers to the new UDM time-varying model including along-wind-diffusion effects, and UDM FDC refers to the UDM finite-duration-correction method; see the UDM theory manual for full details of the underlying theory.

Chapter 9 considers the analytical verification of the UDM AWD formulation for finite-duration releases.

- Section 9.1 includes a derivation of an analytical solution of the UDM dispersion equations applicable to steady-state continuous, horizontal passive dispersion. This includes analytical solutions for both the cross-wind dispersion coefficient $\sigma_y$ and vertical dispersion coefficient $\sigma_z$.

- Section 9.2 includes a derivation of Ermak's FDC equations applicable for an unpressurised passive constant finite-duration ground-level release. This includes an analytical derivation of values for the maximum concentration over all times. Ermak assumes that the cloud moves with the FDC mean convection velocity, which equals the UDM effective speed $u_{eff.}$ In case of a non-constant wind-speed profile, this speed is shown to differ from the UDM cloud speed $u_{cld,}$ with the UDM cloud moving faster than Ermak's cloud.

- Section 9.3 compares Ermak's and UDM equations for concentration c(x,y,z,t) as function of position (x,y,z) and time t for both time-varying and finite-duration releases. The UDM AWD formulation is shown to be more realistic than the FDC formulation, and a full list of differences between the formulations are given. Temporary adjustments to the formulations have been applied to confirm close matching of results of both UDM AWD and UDM FDC formulations with analytical solutions for both average cloud speed and concentration versus time at a given distance.

Chapter 10 considers the verification of the UDM AWD formulation for the case of time-varying releases.

- Section 10.1 includes verification against the time-varying HGSYSTEM 3.0 model HEGADAS-T for the case of dispersion from a pool
- Section 10.2 considers the case of an elevated finite-duration release with rainout (time-varying pool evaporation), and compares concentration predictions between UDM AWD (observer logic; including along-wind diffusion) and the old UDM (segment logic; no along-wind diffusion).
- Section 10.3 considers the case of an elevated time-varying multi-component toxic release from a long pipeline with rainout. This includes comparison of pre-AWD (before and after mass correction), post-AWD and old UDM predictions for both concentrations and doses, and significantly reduced concentrations and doses are shown to be obtained for the new UDM AWD formulations.

# 9 STEADY-STATE AND FINITE-DURATION PASSIVE DISPERSION

## 9.1 UDM model for steady-state passive dispersion

Section 2.2 of the UDM verification manual describes verification for steady-state passive dispersion. This chapter partly repeats some of this section and further expands upon it.

### 9.1.1 Passive-dispersion concentration profile

The UDM passive concentration profile is given by

$$c(x,y,z) = \frac{m_c}{0.5(1+h_d)\pi\, u_a R_y R_z} e^{-\frac{y^2}{R_y^2}} e^{-\frac{(z-z_{cld})^2}{R_z^2}} = \frac{m_c}{(1+h_d)\pi\, u_a \sigma_y \sigma_z} e^{-\frac{y^2}{2\sigma_y^2}} e^{-\frac{(z-z_{cld})^2}{2\sigma_z^2}}$$

Here $m_c$ is the steady-state release rate (kg/s), $u_a$ the wind-speed (m/s) at the cloud centroid height $z_c$ and $\sigma_y=2^{-1/2}R_y$, $\sigma_z=2^{-1/2}R_z$ the empirical passive dispersion coefficients given as a function of x; $z_{cld}$ is the centre-line height with $h_d=0$ for a grounded plume ($z_{cld}=0$) and $h_d=1$ for an elevated plume ($z_{cld}/R_z>>1$). Thus for a ground-level plume the above equation reduces to

$$c(x,y,z) = c_o(x) e^{-\frac{y^2}{2\sigma_y^2}} e^{-\frac{z^2}{2\sigma_z^2}} \quad , \quad with \;\; c_o(x) = \frac{m_c}{\pi\, u_a \sigma_y(x) \sigma_z(x)} \qquad (1)$$

Please note that the above UDM passive profile is applied in the UDM for neutral conditions only (n=2), while for non-neutral conditions n differs from 2. See the UDM theory manual for details.

### 9.1.2 Analytical solution to steady-state passive-dispersion equations

The UDM theory manual includes a complete set of dispersion equations. For isothermal, continuous, horizontal passive dispersion these equations simplify as follows:

- zero water-vapour transfer from ground: $m_{wv}^{gnd}=0$
- no heat transfer from ground: $q_{gnd} = 0$
- horizontal momentum = ambient momentum: $u_{cld}=u_a(z_c)$, $I_x=m_{cld}u_a(z_c)$, $I_{x2}=0$
- zero vertical momentum: $I_z = 0$, $u_z = 0$
- position: $\theta=0$, $dx_{cld}/dt = u_a(z_c)$
- THRM conservation-of-enthalpy equation:
  - $T_{cld}=T_a$
  - density $\rho_{cld}=\rho_a$ → concentration profile m=2
- vertical concentration profile exponent
  - neutral conditions: n=2
  - non-neutral conditions (see equation in Figure 25 in UDM theory manual): n is a function of $H_{eff}$, with $H_{eff} = C_n R_z$ . where $C_n = \Gamma(1+1/n)$
- cloud mass/area relation $m_{cld} = u_a\rho_a A_{cld}(x)$
- cloud area formula
  - n=2: $A_{cld}(x) = (1+h_d)\,\pi\sigma_y\sigma_z$, $h_d=0$ for ground-level
  - general passive: $A_{cld} = 4\, C_m C_n\, \sigma_y\sigma_z\, (1+h_d) = 2(1+h_d)\pi^{1/2} C_n \sigma_y\sigma_z$, where m=2, $C_m = \Gamma(1+1/m) = \Gamma(3/2)=0.5\,\pi^{1/2}$
- cloud mass entrainment: $dm_{cld}/dx = Ent_{pas} = A_{cld}(x)\, u_a\rho_a[\sigma_y^{-1}d\sigma_{ya}/dx+\sigma_z^{-1}d\sigma_{za}/dx]$
- cloud spreading: $dW_{eff}/dx = 0.5(2\pi)^{0.5}\, d\sigma_y/dx = 2^{0.5}\, C_m\, d\sigma_{ya}/dx(x-x_0)$, $C_m = 0.5\,\pi^{0.5}$

Thus two equations remain for $\sigma_y$, $\sigma_z$ [cloud entrainment and cloud spreading equations]:

$$d/dx\,[C_n(1+h_d)\, u_a(z_c)\, \sigma_y\sigma_z] = C_n\,(1+h_d)\, u_a(z_c)\sigma_y\sigma_z[\sigma_y^{-1}d\sigma_{ya}/dx+\sigma_z^{-1}d\sigma_{za}/dx]$$
$$d\sigma_y/dx = d\sigma_{ya}/dx(x-x_0)$$

Using virtual-source distance $x_o=0$, initial $\sigma_y=0$ (true for small release rate), the solution to the second equation equals: $\sigma_y=\sigma_y(x=0)+\sigma_{ya}$. Here $\sigma_y(x=0)$ is the initial value for $\sigma_y$ (see Section 3.2 in UDM theory manual for evaluation of initial data), which may be ignored for a jet release only if the initial plume radius is too small, and for a pool source if the pool source diameter is sufficiently small.

Thus one equation remains for $\sigma_z$ [ignoring $\sigma_y(x=0)$]

$d/dx\ [C_n(1+h_d)\ u_a(z_c)\sigma_{ya}\sigma_z] = C_n(1+h_d)\ u_a(z_c)\ \sigma_{ya}\sigma_z[\sigma_{ya}^{-1}d\sigma_{ya}/dx+\sigma_z^{-1}d\sigma_{za}/dx]$

This equation can be simplified to

$$\frac{d}{dx}\{C_n(1+h_d)u_a(z_c)\sigma_z\} = C_n(1+h_d)u_a(z_c)\frac{d\sigma_{za}}{dx} \quad (2)$$

Where for the case of n=2

$h_d$ = $\mathrm{erf}(z_{cld}/\sigma_z)$

$dh_d/dx$ = $-\ 2\pi^{-0.5}\ z_{cld}\ \sigma_z^{-2}\ d\sigma_z/dx\ /\ \exp[z_{cld}^2/(2\sigma_z^2)] < 0$

Case of uniform wind-speed profile (p=0) and n=2

Using $C_n$ = constant and $u_a(z_c)$= constant, the above equation ( 2 ) further reduces to

$d\sigma_z/dx = d\sigma_{za}/dx - (1+h_d)^{-1}[dh_d/dx]\ \sigma_z$

Thus $\sigma_z \geq \sigma_{za}$:

- For an elevated release in near-field $\sigma_z/z_{cld}<<1$, $h_d\approx1$, $dh_d/dx<<1$ and therefore $\sigma_z\approx\sigma_{za}$. When $\sigma_z$ / $z_{cld}$ approaches 1 (i.e. cloud depth comparable to cloud height, $h_d$ reducing from 1 to 0), $\sigma_z$ starts to become larger than $\sigma_{za}$.
- For a ground-level release, $h_d=0$ and therefore $\sigma_z = \sigma_{za}$

Case of non-uniform wind-speed profile (p>0) and ground-level release ($z_{cld}=0$) and n=2

Using the powerlaw $u_a(z_c) = u_a(z_{ref})\ (z_c/z_{ref})^p$ and Equation ( 23 ), it can be shown that

$u_a^{-1}\ du_a/dx\ = p\ \sigma_z^{-1}[d\sigma_z/dx]$

and therefore the above equation ( 2 ) further reduces to

$(1+p)\ d\sigma_z/dx = d\sigma_{za}/dx$

and therefore (presuming $\sigma_z(x=0)$ is small)

$$\sigma_z = \frac{\sigma_{za}}{1+p} \quad (3)$$

## 9.2 UDM FDC model for finite-duration releases

### 9.2.1 FDC equations (copy of description in UDM theory manual)

The centre-line ground-level concentration $c^{fd}(x)$ at downwind distance x for a constant release with duration $t_{dur}$ is obtained from the steady-state centre-line ground-level concentration $c^{ss}(x)$ by applying a "finite-duration correction":

$$c^{fd}(x) = F\ D\ c^{ss}(x) \quad (4)$$

Here the correction factor F reduces the concentration because of finite release duration $t_{dur}$ (s) and the correction factor D accounts for additional reduction because of averaging the concentrations over an averaging time $t_{av}$ (D=1 in case of no time-averaging):

$$F = erf\left[2^{-3/2}\frac{U_c t_{dur}}{\sigma_x}\right] \quad (5)$$

$$D = \frac{\sqrt{2\pi}\ \sigma_x^t}{U_c t_{av}}\ erf\left[2^{-3/2}\frac{U_c t_{av}}{\sigma_x^t}\right], \quad with \quad \sigma_x^t = \sqrt{\sigma_x^2 + (U_c t_{dur})^2/(2\pi)} \quad (6)$$

Here erf is the well-known error function, $\sigma_x = \sigma_x(x)$ is the downwind dispersion coefficient (m), and $U_c = U_c(x)$ the mean convection velocity of the cloud (m/s).

The downwind dispersion coefficient $\sigma_x = \sigma_x(x)$ consists of two components,

$$\sigma_x(x) = \sqrt{\sigma_{xs}^2(x) + \sigma_{xt}^2(x)} \quad (7)$$

where $\sigma_{xs}$ is the downwind dispersion due to vertical wind shear,

$$\sigma_{xs}(x) = a_{xs}\, x \;, \qquad with \quad a_{xs} = 0.6\, p \left[\frac{0.48}{\gamma}\right]^{p} \tag{8}$$

and $\sigma_{xt}$ is the downwind dispersion due to turbulent spread caused by downwind velocity fluctuations. In the UDM model the formula for $\sigma_{xt}$ is chosen to be equal to the UDM formula for the time-averaged ambient cross-wind dispersion coefficient $\sigma_{ya}$, i.e. $\sigma_{xt}(x) = \sigma_{ya}(x;t_{av})$.

The mean convection velocity of the cloud, $U_c = U_c(x)$, is given by

$$U_c(x) = u_{ref}\left[\gamma \frac{\sigma_z(x)}{z_{ref}}\right]^{p}, \; where \; \gamma = \sqrt{2}\left\{\frac{(1-p\,d)\,\Gamma(\frac{1}{2}p+\frac{1}{2})}{\sqrt{\pi}}\right\}^{1/p} \tag{9}$$

Here the formula for the vertical dispersion coefficient $\sigma_z$ (x) is chosen equal to the UDM formula for the ambient vertical dispersion coefficient, i.e. $\sigma_z$ (x) = $\sigma_{za}$(x), with $\sigma_{za}$(x) given by a stability-class dependent function of x and the surface roughness $z_o$. Furthermore d = $d_{sc}$ + $d_{zo}$ is the exponent in the approximate power-law fit $\sigma_z(x) = (c\, x^d)$. Here c and $d_{sc}$ are a function of stability class, and $d_{zo}$ a function of surface roughness as indicated in the tables below. Thus for example for stability class E and surface roughness 0.01m, Ermak's formula for $\sigma_z(x) = 0.52\, x^{0.7322+0.0523}$.

| Stab. class | A | B | C | D | E | F |
|---|---|---|---|---|---|---|
| c | 0.02 | 0.12 | 0.25 | 0.38 | 0.52 | 0.28 |
| $d_{sc}$ | 0.9021 | 0.8354 | 0.8031 | 0.7614 | 0.7322 | 0.669 |

| $z_0$ (m) | 0.01 | 0.04 | 0.1 | 0.4 | 1 | 4 |
|---|---|---|---|---|---|---|
| $d_{zo}$ | 0.0523 | 0.0255 | 0 | -0.0414 | -0.0625 | -0.079 |

**Table 1. Evaluation of coefficients in power-law for Ermak's vertical dispersion coefficient $\sigma_z$**

Applicability of FDC

A limitation of the above FDC method is that it is strictly speaking only applicable to ground-level non-pressurised constant finite-duration releases without significant rainout. Moreover it produces predictions of the maximum (centre-line ground-level) concentrations only. Therefore it can only be applied for consequence calculations and never for Phast risk calculations. The FDC method was shown by Witlox et al. (2013) to lead to more accurate results than those obtained by the QI method for validation against the Kit Fox experiments involving 20-second releases of $CO_2$ ground-level area sources.

For a finite-duration continuous release, along wind diffusion effects may significantly reduce the maximum concentration for a downwind distance typically larger than $u_a\, t_{dur}$, where $u_a$ is the wind speed and $t_{dur}$ the release duration. Furthermore along-wind diffusion can be ignored during the initial phase of jet dispersion and for heavy clouds (large Richardson number).

## 9.2.2 Derivation of FDC equations – effects of finite-duration

This section contains details on the derivation of the above equations from Ermak[i] (rewritten in UDM notation), presuming no additional time averaging

Time-varying release

For a time-varying source rate Q(t), kg/s, the component mass flow rate $m_c$ (kg/s) passing through a vertical plane (perpendicular to the wind direction) is no longer constant but a function of both downwind distance x and time t. Thus for this case Ermak quotes the following passive dispersion profile (generalised version from the steady-state profile):

$$c(x,y,z,t) = \frac{m_c(x,t)}{\pi U_c(x)\sigma_y(x)\sigma_z(x)}\, e^{-\frac{y^2}{2\sigma_y^2}}\, e^{-\frac{z^2}{2\sigma_z^2}} \tag{10}$$

$$m_c(x,t) = \frac{U_c(x)}{(2\pi)^{1/2}\sigma_x(x)} \int_0^t Q(\tau)\, \exp\left\{-\frac{[x-U_c(x)[t-\tau]]^2}{2[\sigma_x(x)]^2}\right\} d\tau$$

where $U_c$(x) is the mean cloud convection velocity at downwind distance x.

Steady-state release

For the special case of a steady-state release, the release rate Q(t)=$Q_o$ = constant. Applying $t \to \infty$ in Equation ( 10 ), and substituting for the integrand variable s = {x–$U_c$ (t-τ)}/ {$2^{1/2}\sigma_x$}, one obtains

$$m_c(x,\infty) = \frac{Q_o}{\pi^{1/2}} \int_{-\infty}^{x/(2^{1/2}\sigma_x)} \exp\{-s^2\} ds = \frac{Q_o}{2}\left\{erf(\infty) + erf\left(\frac{x}{2^{1/2}\sigma_x}\right)\right\} = \frac{Q_o}{2}\left\{1 + erf\left(\frac{x}{2^{1/2}\sigma_x}\right)\right\} \quad (11)$$

$$with\ error\ function \quad erf(S) = \frac{2}{\pi^{1/2}} \int_0^S \exp\{-s^2\} ds$$

Ermak states that generally x >> $\sigma_x$, and therefore $m_c(x, \infty) \approx Q_o$, and thus Ermak's formula reduces to the UDM passive concentration profile. Physically x >> $\sigma_x$ implies that downwind convective transport dominates downwind turbulent transport for the case of a continuous steady-state plume, i.e. downwind diffusion can be neglected for steady-state plumes.

Finite-duration release

For the special case of a finite-duration release with duration $t_{dur}$, the release rate $Q(t) = Q_o$ for $0<t<t_{dur}$, and $Q(t)=0$, for $t> t_{dur}$. Again we apply in Equation ( 10 ) the above substitution $s = \{x - U_c(t-\tau)\}/\{2^{1/2}\sigma_x\}$ with integration of $\tau$ over the range [0,t] for $0<t<t_{dur}$, and over the range $[0,t_{dur}]$ for $t>t_{dur}$. Thus one obtains:

$$m_c(x,t) = \frac{Q_o}{2}\left\{erf\left(\frac{x}{2^{1/2}\sigma_x}\right) - erf\left(\frac{x-U_c t}{2^{1/2}\sigma_x}\right)\right\},\ 0<t<t_{dur} \quad (12)$$

$$= \frac{Q_o}{2}\left\{erf\left(\frac{x-U_c(t-t_{dur})}{2^{1/2}\sigma_x}\right) - erf\left(\frac{x-U_c t}{2^{1/2}\sigma_x}\right)\right\},\ t>t_{dur}$$

According to the above equation, $m_c$ at a given downwind distance x is zero at time t=0 (start time of release) and subsequently increases with time t until the time $t_{max}$ at which the maximum concentration is achieved. By differentiating the above formula for $t > t_{dur}$ to time t, it can be found that $dm_c(x,t)/dt = 0$ at time $t = x/U_c + \frac{1}{2}t_{dur}$. Thus the time $t_{max}$ is found to be given by

$$t_{max} = t_{dur}, \qquad x < \frac{1}{2}U_c t_{dur} \quad (13)$$

$$= \frac{x}{U_c} + \frac{t_{dur}}{2}, \quad x > \frac{1}{2}U_c t_{dur}$$

Thus the maximum value of $m_c(x,t)$ over all times t is given by

$$m_c^{max}(x) = \frac{Q_o}{2}\left\{erf\left(\frac{x}{2^{1/2}\sigma_x}\right) - erf\left(\frac{x-U_c t_{dur}}{2^{1/2}\sigma_x}\right)\right\}, \quad x < \frac{1}{2}U_c t_{dur} \quad (14)$$

$$= Q_o\ erf\left(\frac{U_c t_{dur}}{2^{3/2}\sigma_x}\right), \qquad x > \frac{1}{2}U_c dur$$

As indicated above generally x >> $\sigma_x$, and for the interval $0 < x < \frac{1}{2}U_c t_{dur}$ also $U_c t_{dur} - x >> \sigma_x$. Thus for practical purposes:

$$m_c^{max}(x) = Q_o, \qquad x < \frac{1}{2}U_c t_{dur} \quad (15)$$

$$= Q_o\ erf\left(\frac{U_c t_{dur}}{2^{3/2}\sigma_x}\right), \qquad x > \frac{1}{2}U_c t_{dur}$$

The F term in the current UDM FDC implementation [see Eq. ( 5 )] is derived from the last term in the above equation and is applied in the UDM for all x values, and therefore not only for $x>0.5U_c t_{dur}$.

UDM effective cloud velocity

Appendix A.2 of the UDM theory manual shows how the UDM approximates the vertical ambient logarithmic profile by a power law $u_a(z) = u_a(z_{ref})\,(z/z_{ref})^p$. Section 3.2 of the UDM theory manual introduces the concept of equivalent 'cloud effective data'. For a ground-level cloud moving with the ambient wind speed $u_a$, the so-called effective cloud velocity $u_{eff}$ is shown to be given by

$$u_{eff}(x) = \frac{\int_0^\infty u_a(z)\,c(x,y,z)\,dz}{\int_0^\infty c(x,y,z)\,dz} = \frac{u_a(z_{ref})}{(p+1)}\left(\frac{R_z}{z_{ref}}\right)^p \Gamma\left(1+\frac{p+1}{n}\right)/\Gamma\left(1+\frac{1}{n}\right), \quad (16)$$

$$with\ gamma\ function \quad \Gamma(S) = \int_0^\infty t^{S-1}e^{-t}\,dt,\ \Gamma(1+S) = S\,\Gamma(1+S),\ \Gamma(\tfrac{1}{2}) = \pi^{1/2},\ R_z = 2^{1/2}\sigma_z$$

For a passive Gaussian plume (vertical concentration profile exponent n=2) the above equation reduces to

$$u_{eff}(x) = \frac{2^{p/2}}{\pi^{1/2}}\Gamma\left(\frac{p+1}{2}\right) u_a(z_{ref})\left(\frac{\sigma_z}{z_{ref}}\right)^p \quad (17)$$

Ermak FDC mean convection velocity

Ermak presumes that the cloud moves with the above effective cloud velocity. By using an approximate power-law fit $\sigma_z(x) = (c\, x^d)$, it follows that

$$\frac{dx}{dt} = u_{eff}(x) = \frac{2^{p/2}}{\pi^{1/2}}\Gamma\left(\frac{p+1}{2}\right) u_a(z_{ref})\left(\frac{c}{z_{ref}}\right)^p x^{d\,p} \quad (18)$$

By separation of variables (x, t) and subsequent integration,

$$\int_0^x \xi^{-dp} d\xi = \frac{2^{p/2}}{\pi^{1/2}}\Gamma\left(\frac{p+1}{2}\right) u_a(z_{ref})\left(\frac{c}{z_{ref}}\right)^p \int_0^t d\tau \quad (19)$$

Thus

$$x^{1-dp} = \frac{2^{p/2}(1-dp)}{\pi^{1/2}}\Gamma\left(\frac{p+1}{2}\right) u_a(z_{ref})\left(\frac{c}{z_{ref}}\right)^p t \quad (20)$$

which can be rewritten as

$$x = \frac{2^{p/2}(1-dp)}{\pi^{1/2}}\Gamma\left(\frac{p+1}{2}\right) u_a(z_{ref})\left(\frac{\sigma_z(x)}{z_{ref}}\right)^p t \quad (21)$$

Thus the mean convective velocity at a downwind distance x (with travel time t to that distance) is given by

$$U_c(x) = \frac{x(t)}{t} = u_a(z_{ref})\left(\frac{\gamma\ \sigma_z(x)}{z_{ref}}\right)^p, \quad with\ \gamma = 2^{1/2}\left\{\frac{(1-dp)}{\pi^{1/2}}\Gamma\left(\frac{p+1}{2}\right)\right\}^{1/p} \quad (22)$$

[Note that for the specific case of p=0 (uniform wind-speed profile) this reduces to $U_c = u_a$]

UDM cloud speed

According to the UDM theory the UDM cloud moves with the speed at the cloud centroid height. According to Section 3.1.1 of the UDM theory manual, the cloud centroid height $z_c$ is given in case of a ground-level plume by

$$z_c(x) = \frac{\int_0^\infty z\, c(x,y,z)\, dz}{\int_0^\infty c(x,y,z) dz} = \frac{\Gamma\left(1+\frac{2}{n}\right)}{\Gamma\left(1+\frac{1}{n}\right)}\frac{\sigma_z}{2^{1/2}}, \qquad general\ n \quad (23)$$

$$= \frac{2^{1/2}\sigma_z}{\pi^{1/2}}, \qquad n = 2$$

In case of a passive ground—level release, the UDM cloud speed is the passive wind-speed at this cloud centroid height given by

$$\frac{dx_{UDM}}{dt} = u_a(z_{ref})\left(\frac{z_c}{z_{ref}}\right)^p \quad (24)$$

$$= u_a(z_{ref})\left(\frac{\Gamma\left(1+\frac{2}{n}\right)}{\Gamma\left(1+\frac{1}{n}\right)}\frac{\sigma_z}{2^{1/2} z_{ref}}\right)^p, \qquad general\ n$$

$$= u_a(z_{ref})\left(\frac{2^{1/2}\sigma_z}{\pi^{1/2} z_{ref}}\right)^p \qquad n = 2$$

Thus the ratio of the UDM cloud speed ( 24 ) and the UDM effective cloud speed ( 16 ) is given by:

$$\frac{dx_{UDM}}{u_{eff}} = \frac{n\left\{\Gamma\left(1+\frac{2}{n}\right)\right\}^{p}\left\{\Gamma\left(1+\frac{1}{n}\right)\right\}^{1-p}}{2^{p}\,\Gamma\left(\frac{p+1}{n}\right)}, \qquad general\ n \qquad (25)$$

$$= r(p),\ with\ r(p) = \frac{\pi^{1/2-p/2}}{\Gamma\left(\frac{p+1}{2}\right)}, \qquad n = 2$$

Figure 32 in the UDM theory manual shows mostly an increase of p with roughness and stability with values of p ranging between 0.05 and 0.6. For both p=0 (constant wind-speed $u_a$) and p=1 (linear profile) the above ratio r(p) = 1, i.e. the effective cloud moves with the same speed as the UDM cloud. For n=2 and 0<p<1 the UDM cloud moves slightly faster than the effective cloud; see Figure 1 which shows a maximum value of the ratio r(p) of 1.087 at p=0.44.

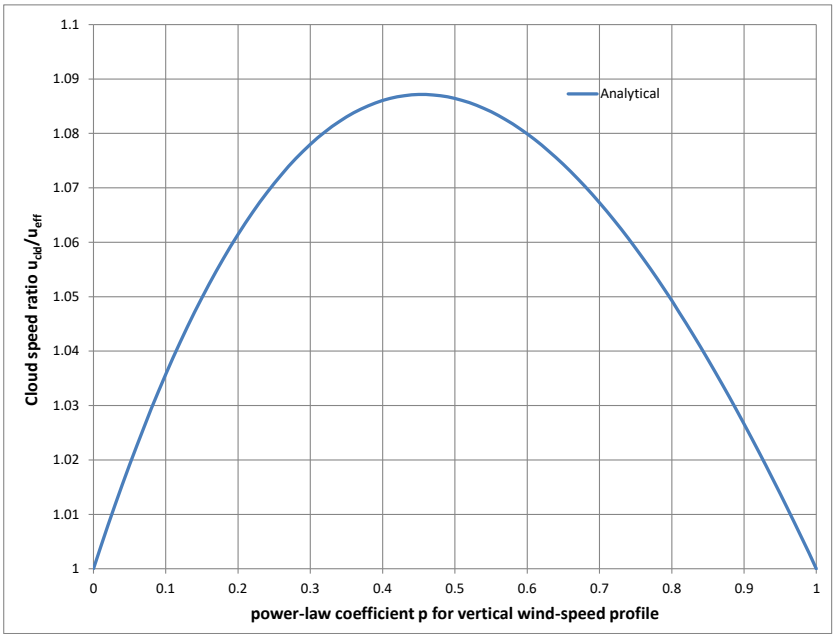


**Figure 1.** **Ratio r(p) of UDM cloud speed and effective cloud speed** [ground-level passive dispersion; n=2]

## 9.2.3 Derivation of FDC equations – effects of additional time-averaging (to add)

TO BE ADDED

Steps;

(a) Integrate concentration over time between t-$t_{av}$ and t+$t_{av}$
(b) Transform dx =$U_c$ dt to convert to integral over downwind distance x
(c) Evaluate this integral analytically to obtain D term

## 9.3 Comparison of UDM FDC and UDM AWD formulations

### 9.3.1 Equations for time-varying and finite-duration releases

General time-varying case

By substituting in the integrand of Ermak's equation ( 10 ) , $\xi = U_c(x)\,(t-\tau)$, the concentration as function of location (x,y,z) and time t can be written as:

$$c(x,y,z,t) = \int_0^{U_c(x)t} \left[ \frac{Q(t-\xi/U_c)}{\pi U_c(x)\sigma_y(x)\sigma_z(x)} e^{-\frac{y^2}{2\sigma_y^2}} e^{-\frac{z^2}{2\sigma_z^2}} \frac{1}{(2\pi)^{1/2}\sigma_x(x)} \exp\left\{-\frac{(x-\xi)^2}{2\sigma_x{}^2(x)}\right\} \right] d\xi = \quad \textbf{( 26 )}$$

$$\approx \int_0^{U_c(x)} \frac{C_{st}(x,y,z;Q(t-\xi/U_c)}{(2\pi)^{1/2}\sigma_x(x)} \exp\left\{-\frac{(x-\xi)^2}{2\sigma_x{}^2(x)}\right\} d\xi \quad , \quad \textit{Ermak FDC formulation}$$

Where $C_{st}(x,y,z;Q)$ is the steady-state concentration at location (x,y,z) based on a steady-state release rate Q.

In the UDM AWD observer formulation it is presumed that the 'observer' released at time $\tau$ observes the flow rate $Q(\tau)$ and the observer concentration is given the corresponding steady-state concentration $C(\xi,y,z;t)= C_{st}(\xi,y,z;Q(\tau))$. The concentration c after inclusion of AWD is given by:

$$c(x,y,z,t) = \int_{\xi_{cld}{}^{uw}}^{\xi_{cld}{}^{dw}} \frac{C(\xi,y,z,t)}{(2\pi)^{1/2}\sigma_x(\xi)} \exp\left\{-\frac{(x-\xi)^2}{2\sigma_x{}^2(\xi)}\right\} d\xi \quad \textbf{( 27 )}$$

$$= \int_{\xi_{cld}{}^{uw}}^{\xi_{cld}{}^{dw}} \frac{C_{st}(\xi,y,z,t;Q(\tau(\xi))}{(2\pi)^{1/2}\sigma_x(\xi)} \exp\left\{-\frac{(x-\xi)^2}{2\sigma_x{}^2(\xi)}\right\} d\xi \ , \ \textit{UDM AWD formulation}$$

The latter expression corresponds to the evaluation of the UDM concentration after effects of along-wind diffusion within the UDM. The upper integral limit $\xi_{cld}{}^{dw}$ is the location of downwind edge of the cloud, corresponding to the position of the observer located most downwind (released at start of release, i.e. at time t=0). The lower integral limit $\xi_{cld}{}^{uw}$ is the location of upwind edge; $\xi_{cld}{}^{uw}$=0 during the release (t < release duration $t_{dur}$), and $\xi_{cld}{}^{uw}$ corresponds to the position of the observer located most upwind (released at end of release, i.e. at time t=$t_{dur}$).

The UDM AWD Equation ( 27 ) slightly differs from the Ermak FDC Equation ( 26 ). The UDM AWD formulation effectively assumes that the concentration at a given location x is governed by mass diffusing away from the surrounding observers [by integration over observer distances ξ; diffusion governed by dispersion coefficient $\sigma_x(x)$]. On the other hand the UDM FDC formulation effectively assumes that the concentration at a given location x is governed only by the observer present at that location, with observer mass diffusing away from this location x governed by dispersion coefficient $\sigma_x(x)$. It is considered that the UDM AWD integration appears to be more realistic than the FDC formulation.

Special case: finite-duration release

For the special case of a finite duration release $Q(\tau)=Q_o$, for $0< \tau<t_{dur}$ the above becomes:

$$c(x,y,z,t) = \int_{\max[\,0,U_c(x)(t-t_{dur})]}^{U_c(x)t} \left[ \frac{C_{st}(x,y,z;Q_o)}{(2\pi)^{1/2}\sigma_x(x)} \exp\left\{-\frac{(x-\xi)^2}{2\sigma_x{}^2(x)}\right\} \right] d\xi \ , \ \textit{Ermak FDC formulation} \quad \textbf{( 28 )}$$

The above equation slightly differs from the UDM formula, which adopts the following equation:

$$c(x,y,z,t) = \int_{X_{st}(\max[\,0,t-t_{dur}])}^{X_{st}(t)} \frac{C_{st}(\xi,y,z;Q_o)}{(2\pi)^{1/2}\sigma_x(\xi)} \exp\left\{-\frac{(x-\xi)^2}{2\sigma_x{}^2(\xi)}\right\} d\xi \ , \ \textit{UDM AWD formulation} \quad \textbf{( 29 )}$$

Here $X_{st}(t)$ is the downwind distance of the downwind edge of the UDM steady-state (pre-AWD) cloud at time t.

Thus there are three subtle differences between the above integrals for Ermak FDC and UDM AWD formulations:

- FDC uses $\sigma_x(x)$, while UDM AWD adopts $\sigma_x(\xi)$
- FDC uses the concentration $C_{st}(x,y,z\,;Q_o)$ which is independent of the integrand variable ξ, while UDM AWD adopts $C(\xi,y,z\,;Q_o)$
- The FDC downwind edge of the cloud irrealistically depends via $U_c(x)$ on both x,t, while the UDM downwind edge of the cloud more correctly depends on t only. For $t>t_{dur}$, likewise for the upwind edge of the cloud.

Thus it is considered that the UDM AWD integration appears to be more realistic than the FDC formulation.

Approximating in ( 29 ), $C_{st}(\xi,y,z;Q_o)$ with $C_{st}(x,y,z;Q_o)$, and $\sigma_x(\xi)$ with $\sigma_x(x)$, and substituting $s = (\xi - x)/(2^{1/2}\sigma_x)$ one obtains:

$$\frac{c_{UDM}(x,y,z,t)}{c_{st}(x,y,z;Q_o)} = \frac{1}{(2\pi)^{1/2}\sigma_x(x)} \int_{X_{st}(\max[0,t-t_{dur}])}^{X_{st}(t)} \exp\left\{-\frac{(x-\xi)^2}{2\sigma_x^{\,2}(x)}\right\} d\xi \quad \textbf{( 30 )}$$

$$= \frac{1}{\pi^{1/2}} \int_{\{X_{st}(\max[0,t-t_{dur}])-x\}/\{2^{1/2}\sigma_x(x)\}}^{\{X_{st}(t)-x\}/\{2^{1/2}\sigma_x(x)\}} \exp\{-s^2\} ds =$$

$$= \frac{1}{2}\left\{ erf\left(\frac{X_{st}(t)-x}{2^{1/2}\sigma_x(x)}\right) - erf\left(\frac{X_{st}(\max[0,t-t_{dur}])-x}{2^{1/2}\sigma_x(x)}\right)\right\}$$

where it is repeated that $X_{st}(t)$ is the travel distance of the steady-state plume at time t.

Note that for a steady-state plume $t_{dur}=\infty$ and using $x >>> \sigma_x$, it can be shown that the above equation reduces to unity as should be the case:

$$\frac{c_{UDM}(x,y,z,t)}{c_{st}(x,y,z)} \approx \frac{1}{2}\left\{ erf\left(\frac{X_{st}(t)-x}{2^{1/2}\sigma_x(x)}\right)+1\right\} \approx 1, \quad for\ t\to\infty\ and\ steady-state \quad \textbf{( 31 )}$$

The above Equation ( 30 ) may be compared with the Ermak FDC equation ( 12 ), and the equations match provided that the UDM would move with the same speed at the UDM FDC cloud, i.e. provided that $X_{st}(t) = t\ U_c(x)$ and $X_{st}(t-t_{dur}) = (t-t_{dur})\ U_c(x)$

## 9.3.2 List of differences between AWD and FDC formulations

Additional assumptions for the FDC formulation (as currently implemented) which may cause differences with the UDM AWD formulation (without additional time-averaging) are as follows:

- Type of release
  - Finite-duration release with uniform release rate
  - Ground-level release (not elevated; no rainout; including vertical wind-speed profile)
  - Passive release (not heavy-gas and jet-dispersion, e.g. heavy-gas cloud may move with a lower speed and jet may move with a faster speed than a passive cloud)
- Cloud speed
  - Ermak's cloud moves with the effective cloud speed and UDM cloud moves with the cloud centroid speed; these speeds are identical for the specific case of passive dispersion, ground-level cloud and uniform wind-speed profile
  - FDC does not presume a cut-off height for wind-speed, while the UDM presumes by default a cut-off height of 1m (but this default value can be reduced)
- Concentration profile
  - Ermak's FDC formulation presumes vertical Gaussian profile exponent n=2, while the UDM value for n differs from 2 in case of non-neutral conditions.
- Passive dispersion coefficients $\sigma_{ya}$, $\sigma_{za}$
  - Values at x=1m are adopted in the UDM for 0<x<1. In case of passive dispersion there will be in addition further differences in the near-field between $\sigma_{ya}$, $\sigma_{za}$ and $\sigma_y$, $\sigma_z$, because of (a) the initial source size (case of a jet) and (b) passive dispersion must be downwind of the pool source (case of a pool source). Furthermore the UDM calculated value for $\sigma_z$ is only equal to $\sigma_{za}$ in case of a sufficiently elevated cloud and/or in case of a uniform wind-speed profile. E.g. for a ground-level passive release $\sigma_z = (1+p)\ \sigma_{za}$, where p is the wind-speed power-law exponent
  - Ermak's original FDC derivation for the mean convection velocity $U_c$ [see Equation ( 22 ) ] is based on a power-law fit for FDC vertical dispersion coefficient $\sigma_z = cx^d$, while the actual UDM FDC implementation accounts for the d value but adopts the UDM $\sigma_z$ in the remaining formula for the convection velocity, which is not fully correct. For example for stability class E, $z_o$=0.01m
    - original Ermak FDC formula: $\sigma_z^{FDC}(x) = 0.52x^{0.7322+0.0523} = 0.52x^{0.7845}$
    - Vertical dispersion UDM formula $\sigma_{za}(x)$ (see Section 3.4.5 of UDM theory manual) given by Hosker formula (linearly varying up to 100m and later on different). Thus according to Equation ( 3 ) the actual calculated UDM $\sigma_z(x) = \sigma_{za}(x)/(1+p)$. For 0<x<100m: $\sigma_z^{UDM}(x) = 0.0237x/(1+p)$
    - In the current UDM FDC formulation
      - d = 0.7845

- $\sigma_z(x)=\sigma_{za}^{UDM}(x)$ = original Hosker value

Thus to ensure full consistency of UDM convection velocity between FDC and UDM AWD, the following assumptions should be made instead inside the FDC routine for the evaluation of the mean convection velocity:

- d=1
- $\sigma_z(x)=\sigma_{za}^{UDM}(x)/(1+p) = 0.0237x/(1+p)$
- Apply existing Equation ( 22 ) to set $U_c$
- Set $U_c = r(p)\, U_c$, to ensure consistency of cloud speed in FDC routine and UDM speed

Figure 2 shows Ermak's values for $\sigma_z$ much larger than the UDM Hosker values. However a larger value of $\sigma_z(x)$ results into less reduction of concentrations in the vertical direction, and therefore a larger value of the convection velocity. This could be resolved by changing c,d in FDC formula such as to match linear law upto 100m (but this will result in differences for x>100m), i.e. use FDC $\sigma_z(x) = 0.0237x$ (see FDC modified curve below).

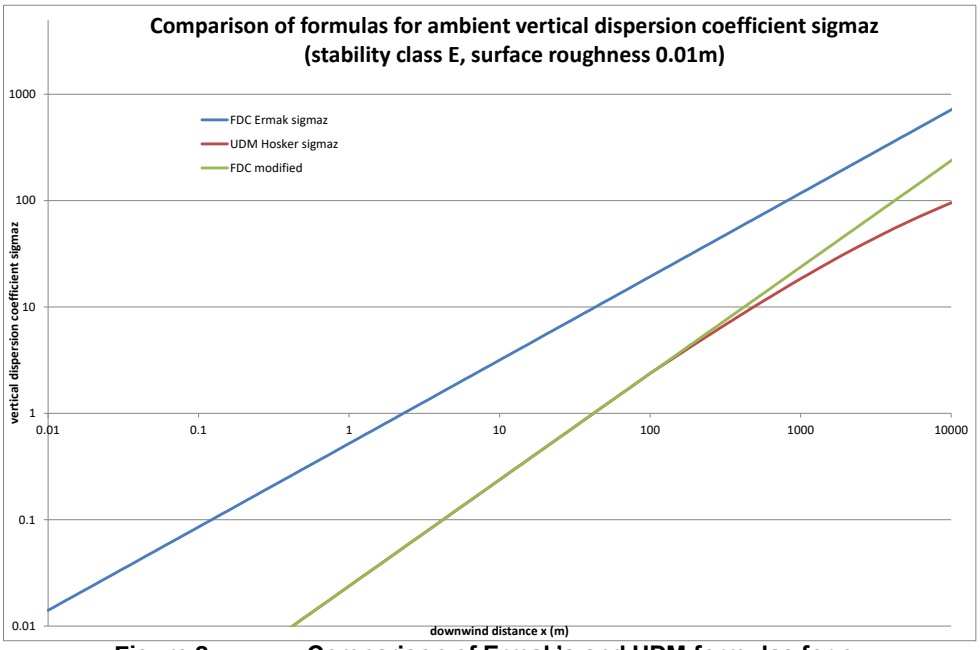


**Figure 2. Comparison of Ermak's and UDM formulas for $\sigma_z$**

- Additional model differences between AWD and FDC formulations
  - FDC assumes $x>>\sigma_x$
  - There are several discrepancies between the FDC and UDM AWD integration of of the steady-state concentrations to include AWD effects, i.e.
    - FDC evaluates in integral dispersion coefficients as function of downwind distance x, while AWD evaluates dispersion coefficients as function of integrand variable ξ
    - FDC uses the concentration $C_{st}(x,y,z\,;Q_o)$ which is independent of the integrand variable ξ, while UDM AWD adopts the observer concentration $C(\xi,y,z\,;Q_o)$
    - The FDC downwind edge of the cloud irrealistically depends via the mean convection velocity $U_c(x)$ on both x and t, while the UDM downwind edge of the cloud more correctly depends on t only. For $t>t_{dur}$, likewise for the upwind edge of the cloud

### 9.3.3 Verification of UDM AWD results against analytical and FDC results

A test case was set up for ground-level passive dispersion (weather E2, zero humidity, averaging time 20s, release duration 10 seconds or steady-state), with 'dry air' being released.

Adjustments to UDM input and UDM code

The following correction/adjustments were applied to ensure matching of results with analytical solutions.

1. Steady-state passive dispersion

a. Apply low release rate $Q_o = 10^{-5}$ kg/s as well as low initial jet/pool-source diameter (derived from velocity). This has been applied to ensure early passive transition (upwind of 0.1m) and to obtain matching of vertical and crosswind dispersion coefficients in the near field.
b. Modified non-default parameter input: set cut-off height for ambient velocity to 1cm instead of 1m
c. Temporary code changes:
    i. Stability classes E,F apply value n>2 in UDM and to align Ermak theory use temporarily n=2 for these stability classes to ensure matching
    ii. Remove setting $\sigma_y$, $\sigma_z$ for 0<x<1m to values at x=1m

2. Additional temporary code changes for finite-duration releases:
    a. UDM FDC logic
        i. Apply d=1 for power-law fit formula c $x^d$ for $\sigma_z$ (x), for consistency with current UDM $\sigma_z$ evaluation for 0m<x<100m
        ii. According to Equation ( 3 ), apply $\sigma_z$ (x)=$\sigma_{za}^{UDM}$(x)/(1+p) instead of $\sigma_z$ (x)=$\sigma_{za}^{UDM}$(x)
        iii. According to Equation ( 25 ), further modify evaluation of average convection speed $U_c$(x) with additional multiplication factor r(p), to ensure that the adopted convection speed by UDM FDC logic is identical to the UDM cloud speed
    b. AWD – changes to obtain integrand in AWD consistent with that of FDC [cf. Equations ( 26 ) and ( 27 )]
        i. Apply $\sigma_x$(x) in integrand for AWD calculations instead of $\sigma_x$(ξ)
        ii. Use integrand-variable independent concentration C(x,y,z,t) for AWD rather than C(ξ,y,z,t)

<u>Passive testcase with uniform wind-speed (p=0)</u>
For this case very close agreement between UDM numerical results and analytical results were obtained for the steady-state dispersion:

- UDM $\sigma_z$ = analytical value $\sigma_{za}$ (coded up in Excel spreadsheet)
- UDM $\sigma_y$ = analytically value $\sigma_{ya}$ obtained value (coded in spreadsheet)
- Confirmed value of UDM cloud centroid height is identical to Equation ( 23 )
- Confirm UDM centroid speed = $u_a$
- UDM steady-state G/L max. conc. (kg/m$^3$) equals analytical value:

$$c(x,y,z,t) = \frac{Q_o}{\pi u_a \sigma_y(x)\sigma_z(x)} \qquad \textbf{( 32 )}$$

For the 10s finite-duration release (no additional time-averaging) AWD and FDC results were found to be identical; see plot below.

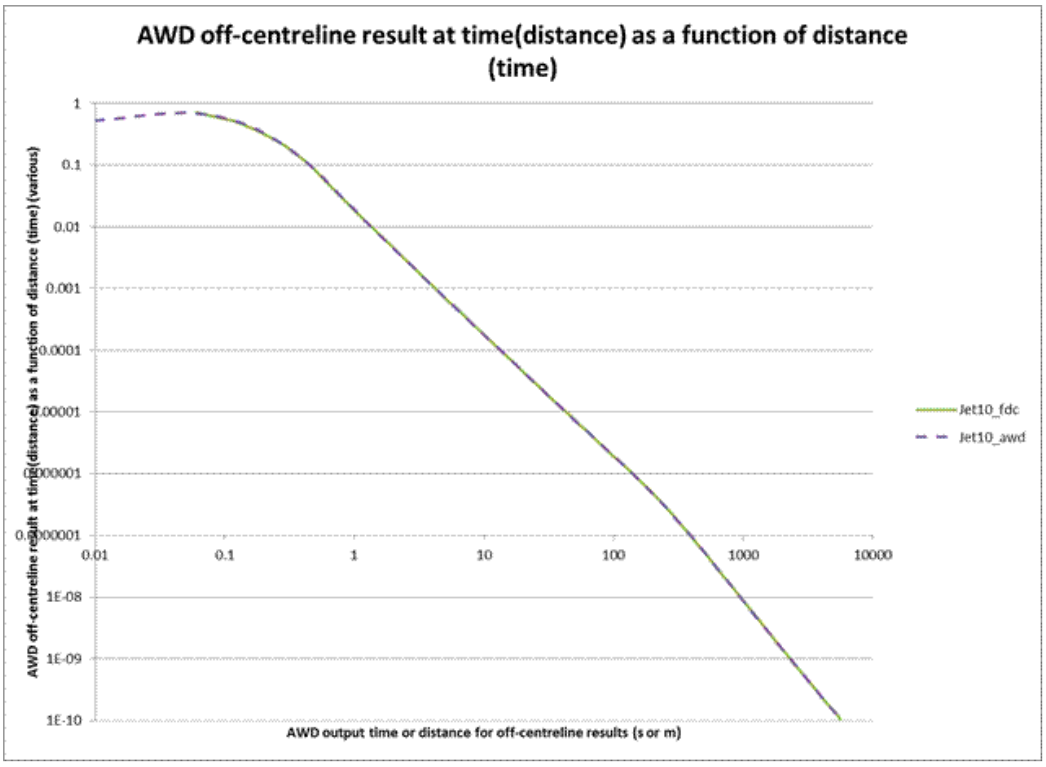


**Figure 3. AWD versus FDC predictions (10s passive release; uniform windspeed)**

Passive test case with default wind-speed profile (p>0) – steady-state release

For weather E2 (stability class E, wind speed of 2m at 10m height), surface roughness 0.01m, the wind-speed power-law exponent p = 0.30494 was found, corresponding to a ratio of UDM cloud speed and Ermak effective speed of r(p)=1.078.

Very close agreement between UDM numerical results and analytical results were obtained for the steady-state dispersion:

- Confirmed that UDM $\sigma_z$ close to analytical value $\sigma_{za}$ / (1+p)
- Confirmed that UDM $\sigma_y$ close to analytical value $\sigma_{ya}$
- Confirmed UDM cloud centroid height $z_c$ identical to Equation ( 23 )
- Confirmed UDM centroid speed = $u_a(z_c)$, as given by Equation ( 24 ); confirmed that $u_{cld}/u_{eff}$ = r(p) = 1.078, with $u_{eff}$ evaluated using Equation ( 16 ) and r(p) using Equation ( 25 )
- Confirmed UDM $\sigma_y$ = analytically obtained value $\sigma_{ya}$ (directly from UDM theory manual; needs small source rate and small initial diameter)
- Confirmed UDM $\sigma_z$ = analytically obtained value =$\sigma_{za}$ / (1+p), where $\sigma_{za}$ is the Hosker vertical passive dispersion coefficient [needs small source rate]
- Confirmed that UDM steady-state G/L max. conc. (kg/m$^3$) equals analytical value:

$$c(x,y,z,t) = \frac{Q_o}{\pi u_a \sigma_y(x)\sigma_z(x)} == \frac{(1+p)Q_o}{\pi u_a(z_c)\sigma_{ya}(x)\sigma_{za}(x)} \qquad (33)$$

- Confirmed that UDM steady-state G/L max. conc. (kg/m$^3$) equals analytical value:

For the 10s finite-duration release (no additional time-averaging) the following is observed:

- Confirmed that the FDC convection velocity $U_c(x)$ after adjustment in the FDC routine with the factor r(p)=1.0758 closely[1] matches the averaged UDM cloud velocity $u_{cld}/t$; see Figure 4.

[1] IMPROVE. For AWD and FDC the downwind integral limits are $X_{st}(t)$ and t $U_c(x)$, respectively, while $X_{st}(t\text{-}t_{dur})$ and $(t\text{-}t_{dur})$ $U_c(x)$ are the upwind integral limits. Ideally a figure would be added which would plot these four curves on a plot in order to further understand the differences (why there is not an exact match) between UDM and AWD results show in Figure 4.

- For AWD the analytical ratio in Equation ( 30 ) can be evaluated for given (x,t) and multiplied with the steady-state concentration $c_{st}$ to evaluate the maximum concentration c(x,0,0,t). Similarly Equations ( 12 ) and ( 11 ) can be used to calculate an analogous ratio for FDC. Figure 5 includes analytical and numerical solutions for AWD and FDC at 900m downwind as a function of time (with UDM AWD and UDM FDC adjustments as given above). It is seen that the FDC analytical time-dependent concentration is correctly capped by the maximum UDM FDC concentration, and the UDM AWD analytical predictions closely match the UDM AWD numerical predictions. Thus this confirms the corrections of the numerical AWD integration.

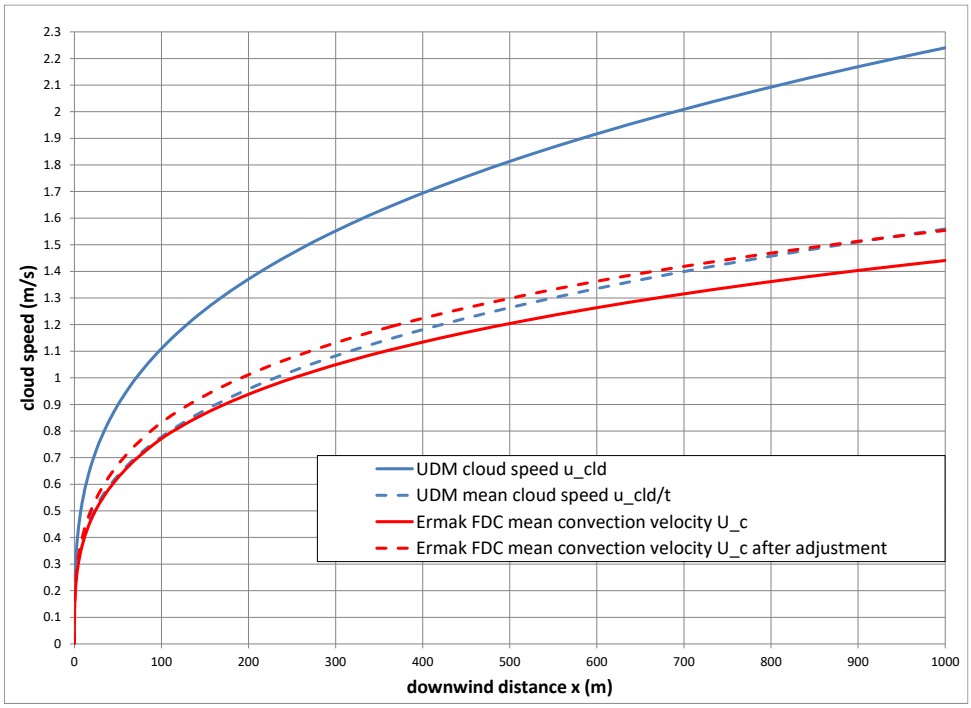


**Figure 4. UDM speed, UDM average speed versus FDC convection speed (10s passive release)**

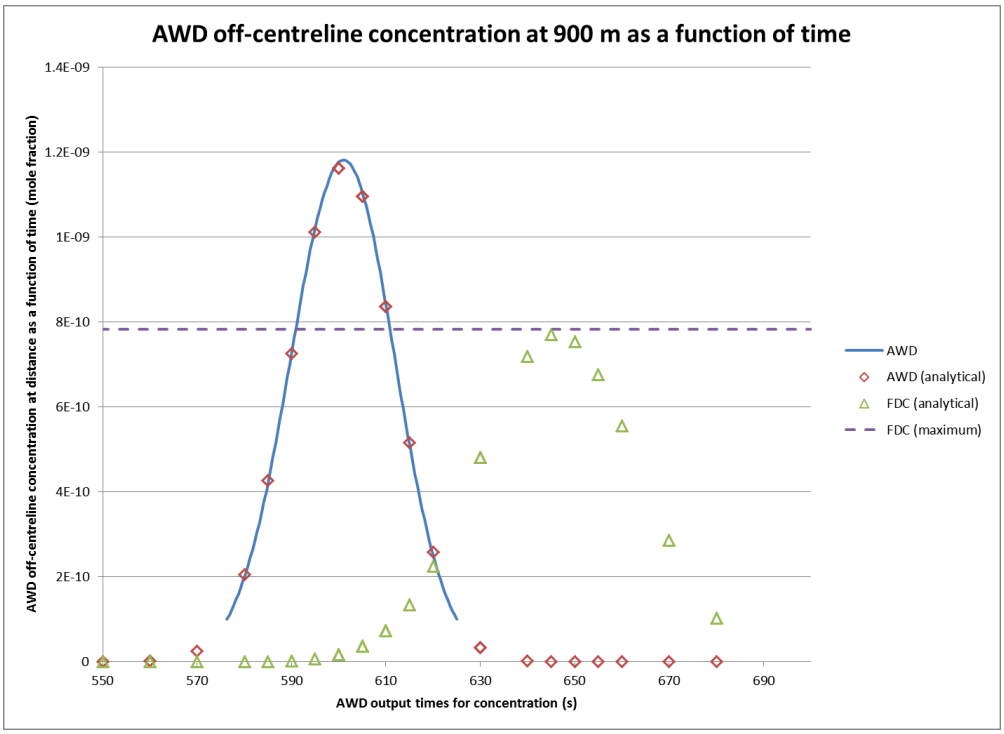


**Figure 5. Analytical verification of AWD and FDC calculations**

# 10 VERIFICATION AND TESTING FOR TIME-VARYING DISPERSION

## 10.1 Dispersion from pool: UDM verification against HGSYSTEM

The case of an instantaneous spill of 10000 kg of butane liquid is considered with both cases of a bund (radius 10m) and no bund (pool on water; dispersion over land). Ambient data applied are stability class D, wind speed at 10m height of 5m/s, temperature 300K and humidity 70%. Furthermore a maximum pool duration of 1 minute is applied, and thus no pool evaporation is assumed to occur after 1 minute.

Figure 4 shows the values predicted by the UDM of butane pool radius and evaporation rate for both cases with and without a bund. It is seen that the immediate butane rainout within the bund results in a virtually steady-state pool of 10 meter radius, 12.3 kg/s evaporation rate and a temperature of 271.8K.

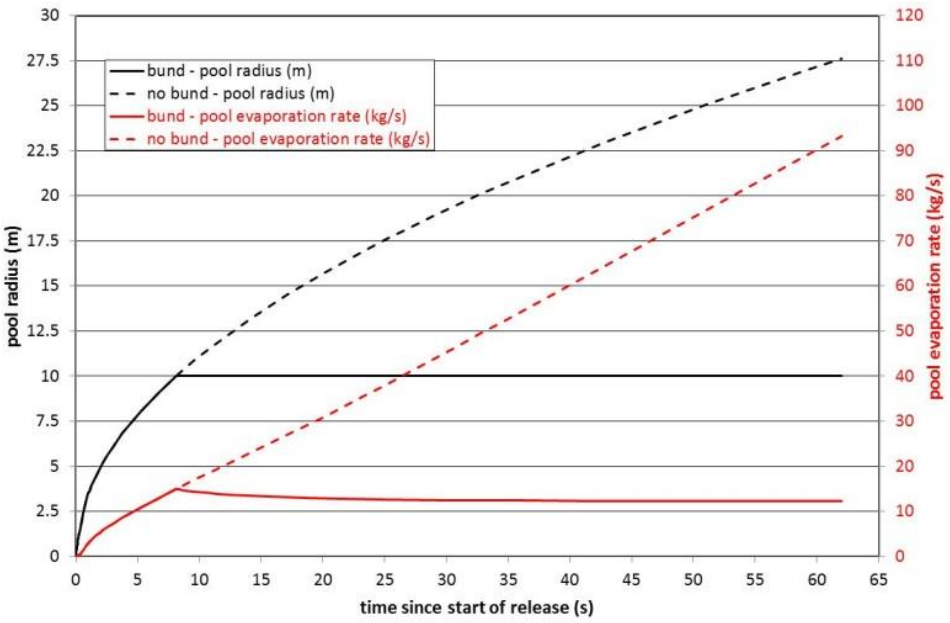


**Figure 4. UDM pool predictions (instantaneous 10000kg spill of butane on water)**

Figure 5 includes results of the following calculations for the case of a bunded pool:

- HGSYSTEM 3.0 calculations (the rectangular HEGADAS source was chosen to be square with the same area as the UDM pool)
  - steady-state HEGADAS-S calculations (ground-level steady-state heavy-gas dispersion from area source) based on the steady-state pool data mentioned above.
  - FDC finite-duration correction (using Ermak's formula) to above HEGADAS-S results (60 seconds duration) using the post-processor program POSTHS
  - HEGADAS-T calculations (ground-level time-varying heavy-gas dispersion from area source). In line with the new UDM model, no gravity-shape correction was applied and the along-wind-diffusion coefficient was chosen to be based on Ermak's formula (non-default HEGADAS-T options)
- UDM calculations
  - Steady-state UDM calculations based on the above steady-state pool data
  - FDC correction to the above steady-state UDM results (60 seconds duration)
  - UDM AWD calculations, with 30 observers released from the upwind edge of the pool

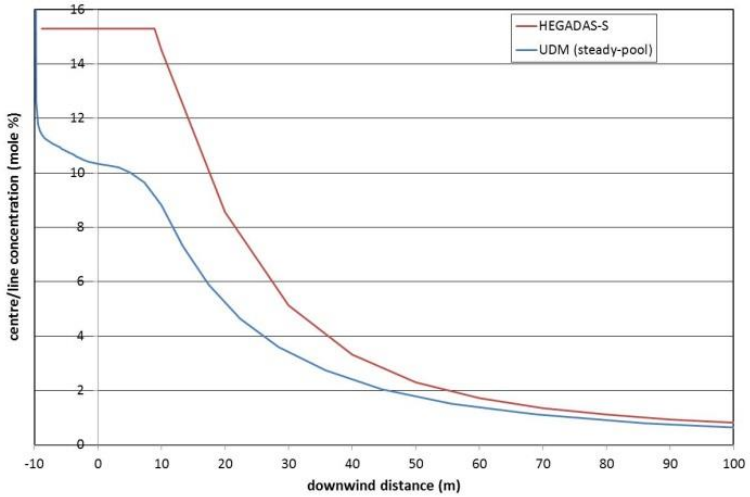


(a) Near-field centre-line concentrations

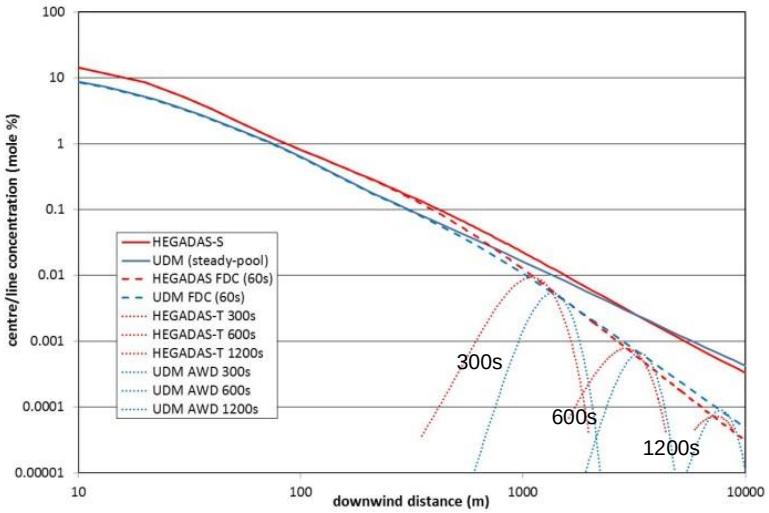


(b) Far-field concentrations

(c)

**Figure 5. UDM verification against HEGADAS for spill of butane with bund (radius 10m)**

Figure 5a includes the steady-state HEGADAS-S and UDM results of the centre-line ground-level concentrations in the near-field for the case of a steady-state pool. HEGADAS-S assumes a uniform concentration (top-hat profile) above the area source (about 15% mole fraction), which is envisaged to lead to an over-prediction near the source. On the other hand, the UDM model more rigorously solves the dispersion equations across the pool allowing for a variation of the concentration across the pool. The very rapid decrease predicted by the UDM of the concentration near the upwind edge of the pool is a numerical artefact and may not occur in reality. Further downwind from the pool a closer match is observed between the UDM and HEGADAS-S data.

Figure 5b includes results of all the above calculations. It includes results of the time-varying dispersion calculations by UDM AWD and HEGADAS-T at output times 300s, 600s and 1200s. It is seen that the maximum values of these curves correctly touch the maximum centre-line concentration (maximum value over all times) predicted by UDM FDC and HEGADAS-S FDC, respectively. This confirms that the AWD integration is carried out correctly by both programs and is consistent with the FDC formulation. Also adequate agreement between the UDM and HEGADAS FDC results is observed. It is seen that initially the HEGADAS-T cloud is more heavy (larger concentrations) and therefore moves more slowly than the UDM AWD cloud, but this effect reduces in the far-field when the predictions become closer.

Likewise, Figure 6 includes UDM AWD and HEGADAS-T results at times 300s, 600s and 1200s for the case without the bund. Here the UDM calculated pool data were specified as input to HEGADAS-T with a step size of 2 seconds. The observed differences are confirmed to be very similar to that seen for the case with the bund (compare Figures 5b and 6).

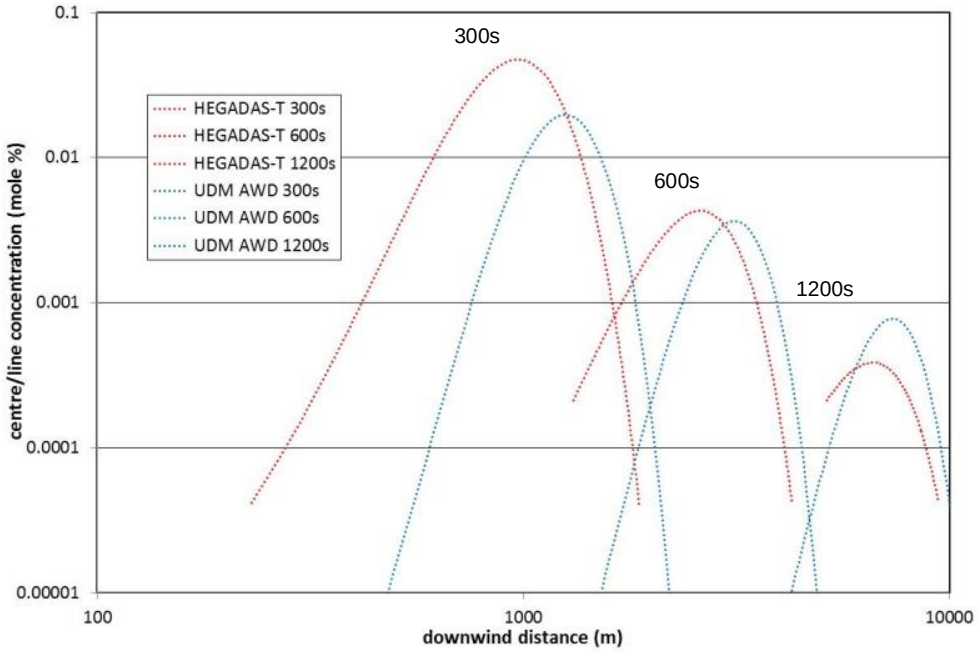


**Figure 6. UDM verification against HEGADAS for spill of butane without bund**

## 10.2 Elevated chlorine release with rainout

This section includes results for a horizontal chlorine release at elevation height of 1m with a constant release rate of 100kg/s for a duration of 50 seconds. The post-expansion data are chosen to correspond with 100% liquid chlorine at its boiling point (213.9K) with a release velocity of 10m/s and an initially presumed SMD droplet size of 0.001m. Ambient data applied were stability D5, temperature 298K and humidity 70%. Furthermore a maximum pool duration of 500 seconds was applied, and thus no pool evaporation is assumed to occur after 500 seconds. Two observers were released from the release point (at start and end of the release) and subsequently 30 observers were released from the pool.

About 90% rainout was predicted at about 5m downwind distance from the release point. Figure 7a shows the values predicted by the UDM of radius and evaporation rate for the un-bunded chlorine pool (pool duration of 500s). The pool radius and evaporation rate are seen to increase rapidly until about 55s at which time the minimum pool thickness is reached. Following this the pool breaks up into wet spots modelled in the UDM by a reducing effective pool radius. The pool evaporation is terminated at the maximum pool duration of 500s.

Figure 7b includes results of both observer concentrations (prior to inclusion of AWD effects; dashed curves) and concentrations after inclusion of AWD effects (solid curves) at output times of 300s, 600s, 1000s and 1500s. Also results are included using the Phast 6.7 UDM segment method (dotted curves). At 300s the release is still on-going, and therefore AWD effects are seen to be only pronounced at the downwind edge of the cloud. With increasing cloud travel times, AWD effects erode concentrations at the upwind and downwind edges of the cloud and increase its cloud length. The pre-AWD observer concentrations predicted by the new UDM observer method are seen to be comparable with the discontinuous segment concentrations predicted by Phast 6.7. Released observers observe a very rapidly reducing discharge rate from the start of the release and this explains the increase of pre-AWD concentration with distance shown in Figure 7b near the downwind edge of the cloud. The new UDM method predicts reduced post-AWD concentrations which are considered to be more accurate. Note that while the AWD cloud at 1500s appears to be

much larger than its pre-AWD equivalent, the concentration scale is logarithmic and mass is conserved between the two methods.

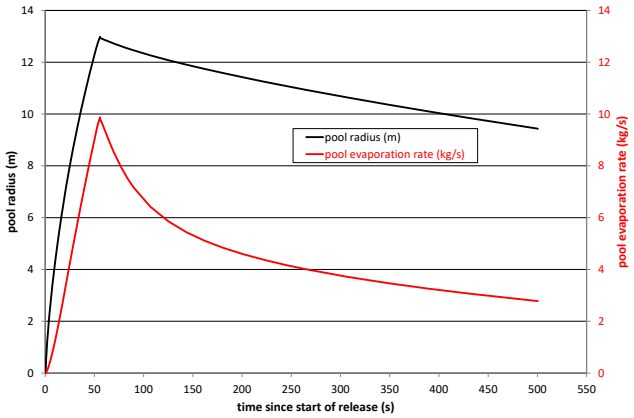


(a) Pool radius and pool evaporation rate

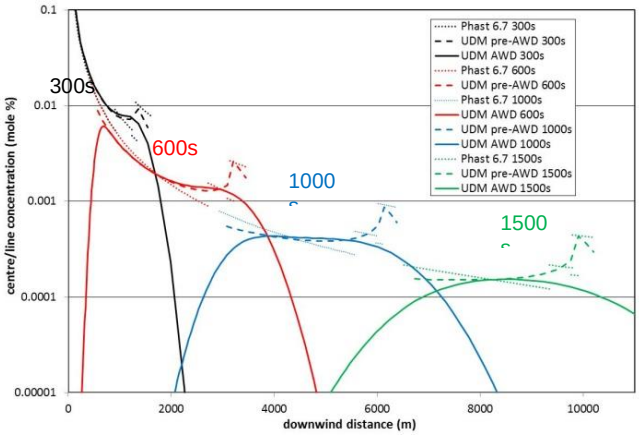


(b) concentrations

**Figure 7. UDM AWD predictions for elevated $Cl_2$ release with rainout**

## 10.3 Elevated sour-gas release from long pipeline without rainout

The example is considered of the time-varying dispersion arising from the time-varying discharge of a sour-gas mixture (including hydrogen sulphide, H2S) from a long pipeline; see Figure 8.

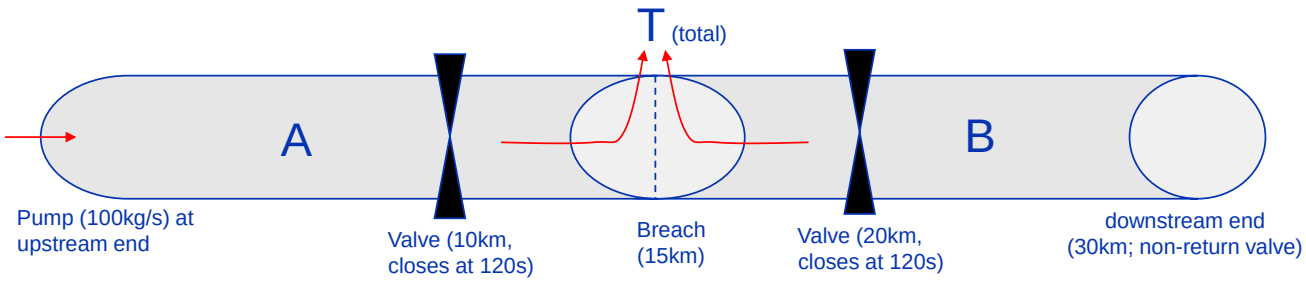


**Figure 8. Schematic figure illustrating pipe geometry and breach/valve locations**

Input data

Input data are selected corresponding to a long pipeline representative of some extremely sour fields found in the Middle East that are now being developed.

The molar composition of the sour-gas mixture is chosen as follows: $CO_2$ (10%), $H_2S$ (35%), methane 50%, ethane 1.5%, propane 1.5%, butane 1% and pentane 1%. This corresponds to a molecular weight of 26.77 kg/kmol. The release is presumed to occur following a full-bore rupture at the middle of a 30km long pipeline (inner diameter 30", roughness 45.7µm typical for carbon steel), with a normal production rate of 100 kg/s and with line block valves (LBVs) located at 10km and 20km from the upstream end (closing at 120 seconds). Prior to the breach the mixture temperature inside the pipe is presumed to be 60°C and the upstream pressure 70barg, where the pressure is defined by the receiving plant Acid Gas Removal Unit's ideal operating conditions.

Selected ambient data input to the UDM dispersion calculations are a temperature of 35°C, a pressure of 1 atm., humidity 60% and weather class D5 (neutral conditions, wind speed 5m/s at 10m height). The selected surface roughness is 1.3cm and an averaging time of 600s was adopted for inclusion of effects of wind-meander for far-field passive dispersion.

High-risk sour gas pipelines are normally buried to minimize the risk of external interference and a rupture would create a crater but for simplicity and to demonstrate the difference between the UDM methods the pipeline has been assumed to be routed above ground.

Discharge calculations; evaluation of observer release data

The Phast model GASPIPE was used to calculate the time-varying discharge rate from the pipe. Here the GASPIPE model models the sour-gas mixture as a non-ideal gas; see the GASPIPE theory manual for details (Webber, Witlox and Stene, 2011). Here the total discharge rate (T) is obtained from summing the discharge rates form the upstream branch A and the downstream branch B. It is conservatively presumed that this results in a single plume with horizontal release direction at 1m elevation height. Default Phast parameters were presumed otherwise for the GASPIPE calculations except that conservation of momentum was assumed (for expansion from breach pressure to ambient pressure) and no velocity cut-off was applied for the post-expansion velocity.

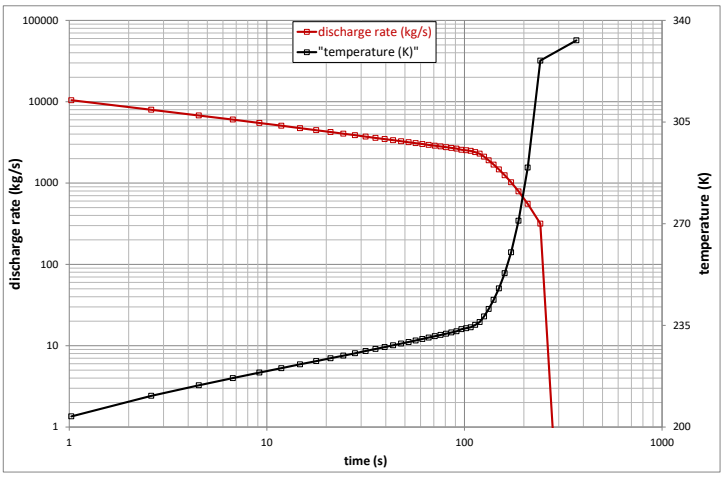


**Figure 9. GASPIPE predictions for time-varying discharge from sour-gas long pipeline**

Figure 9 includes results of GASPIPE predictions of the total time-varying discharge rate and the post-expansion temperature. Initially the pressure immediately upstream of the breach is significantly larger than the ambient pressure, and therefore the subsequent depressurization to ambient pressure results in significantly cold plumes (colder than ambient air; touching down on the ground), while for the final times no cooling occurs resulting in a hot plume of 60°C (slightly lighter than ambient air; rising in the air). 41 observers were chosen to be released based on 40 equal discharge mass segments, and the markers in Figure 9 indicate the corresponding observer data.

## Dispersion results – concentration predictions

The new UDM AWD algorithm (Section 2) was applied based on the release data for the above 41 observers, while the old Phast 6.7 UDM method (Section 1) was applied based on 10 equal-mass segments.

Figure 10 includes results for the predicted ground-level concentration of the sour-gas mixture versus distance (at times 0.5, 1, 2 hours) and time (at distances 5, 10, 20 km). The old Phast 6.7 results (discontinuous segments) are indicated by blue curves, while the new UDM results are given by red curves (at 0.5 hour or 5 km), black curves (at 1 hour or 10 km) or purple curves (at 2 hours or 20 km). The observer concentrations prior to mass correction are indicated by dashed curves with the markers in Figure 10a indicating the location of the observers. Observer concentrations after inclusion of the mass correction are indicated by dotted curves. The concentrations after inclusion of both AWD and mass correction effects are indicated by solid curves, and these are obtained by means of Gaussian integration over the observer concentrations; see Equation (1).

Figure 10 shows that the Phast 6.7 segment predictions (blue curves) are very close to the new UDM pre-AWD predictions before mass correction. In this example the release rate for consecutive segments reduces rapidly, the cloud segment dilutes faster and therefore moves slower resulting in gaps between segments which increase with time and distance downwind. This gap ensures that mass is conserved, but in reality the cloud would not exist as a discontinuous sequence of segments – concentrations would be lower but continuous and therefore concentrations (and other results sensitive to concentration) will be over-estimated in Phast 6.7. It is this effect that the mass correction factor simulates. Uncorrected observer concentrations are in very close agreement with Phast 6.7, but interpolating continuously between these concentrations will effectively create additional mass in the cloud – it is analogous to having Phast 6.7 segments without the gaps. The mass correction reduces concentrations significantly, and this reflects the along-wind 'stretching' of the cloud as early observers travel faster downwind than later ones. It should be noted that the

correction illustrated in this example is very large due to the highly time-varying nature of the release.

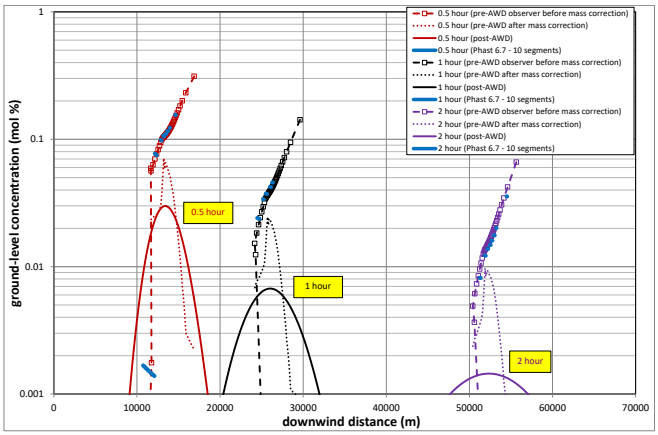


(a) concentration versus distance at 0.5, 1 and 2 hours

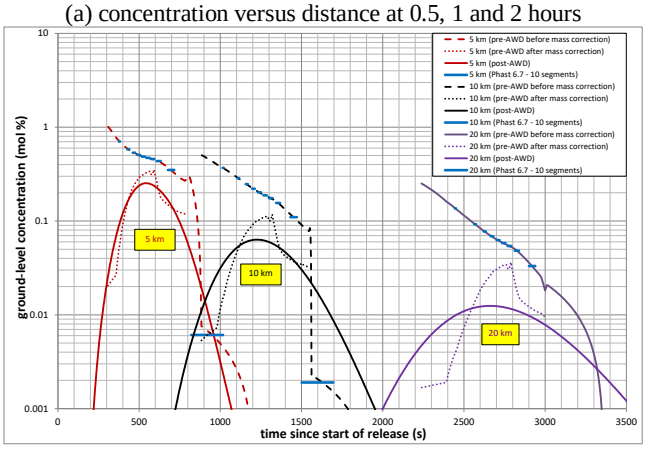


(b) concentration versus time at 5, 10 and 20km

**Figure 10. UDM predictions of ground-level sour-gas mixture concentration**

The discussion so far has excluded any consideration of along-wind diffusion, shown by the solid lines in Figure 10 It too reduces concentrations and elongates the cloud, but it is important to recognize that it models a different physical process, and frequently will have a much more significant effect than mass correction (e.g. for continuous finite-duration releases).With increasing cloud travel times AWD effects erode concentrations at the upwind and downwind edges of the cloud, and increase cloud length (Figure 10a) or passage time for a particular distance (Figure 10b). AWD is more effective at reducing concentrations as distance increases. AWD effects are not included by the Phast 6.7 segment method and therefore this method produces conservative results.

Dispersion results – dose predictions

Figure 11 includes pre-AWD (before and after mass correction) and post-AWD results of the ground-level dose (toxic load D) which is derived by means of integration of UDM concentrations over time,

$$D = \int \left(f_{H2S} c\right)^N dt \qquad (34)$$

Here $f_{H2S}$=0.35 is the mole fraction of toxic $H_2S$ in the sour-gas mixture, and c = c(x,y=0,z=0;t) is the ground-level concentration (ppm). N is a material-specific probit parameter. Figure 11 also includes doses associated with levels published online by the UK HSE (2013), i.e. SLOD (significant likelihood of death; 50% mortality) and SLOT (specified level of toxicity; 1% mortality); HSE adopts a value of N=4 and therefore this has been applied in the current

calculations. In addition Figure 11 includes doses derived from Acute Exposure Guideline Levels AEGL3 (mortality may occur) and AELG2 (irreversible effects) as issued by the USA EPA (2012).

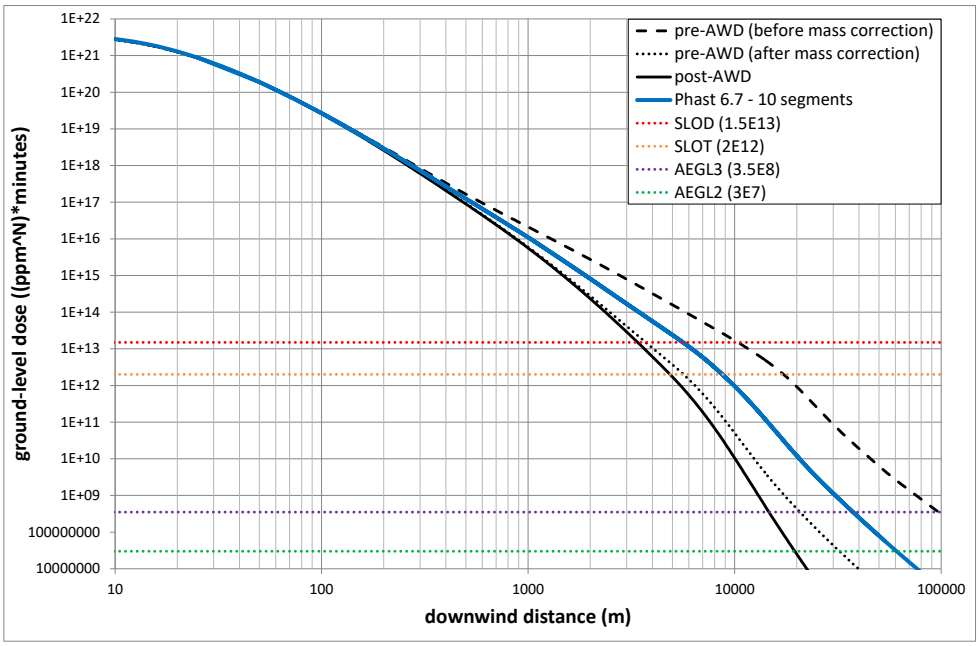


**Figure 11. UDM predictions of dose versus downwind distance**

Figure 11 demonstrates that in the near-field (up to around 300m), gaps between the Phast 6.7 segments are small and also mass-correction and AWD effects are limited, and therefore all dose results match each other closely.

Further downwind, however, the doses start to diverge. Before the mass correction is applied, the doses are greater than those of Phast 6.7. This indicates that the observers are drifting apart and the cloud elongating. As a consequence additional mass is created which accounts for the increased dose. The mass-corrected dose on the other hand is less than the Phast 6.7 dose. This is because there is a non-linear relationship between concentration and dose – i.e. the N value in Equation (11) is > 1 and dose will be highly sensitive to concentration. The Phast 6.7 approach uses segments with gaps in-between and, as already discussed, this will mean that concentrations and therefore doses are too high since N is larger than 1. Using the reduced value of N=1 it was confirmed that toxic dose results are virtually identical between Phast 6.7 and the pre-AWD results after mass correction, since both methods ensure conservation of cloud mass. Further downwind AWD effects lead to a further reduction in dose, and the magnitude on this effect increases with distance downwind.

For other scenarios where the Phast 6.7 mass release rate reduces less rapidly between subsequent observers and segments and where the duration is relatively short, the mass correction effects would be expected to be less significant and the AWD effects relatively more significant. The authors consider that the newly proposed less conservative UDM approach including mass-correction and AWD effects is preferable for predicting toxic loads associated with toxic releases.

# 11 VERIFICATION AND TESTING OF GRAVITY SHAPE CORRECTION

The gravity shape correction is carried out following the initial observer calculations. It reduces the incremental cloud width and increases the incremental cloud length, such that cloud area is conserved, and such that gravity spreading in the downwind direction is the same as gravity spreading in the crosswind direction; see the UDM theory manual for further details.

It is currently applied as follows for an individual observer:

- Only applied downwind of jet/heavy transition and downwind of the downwind edge of the pool; only applied upwind of the start of transition to passive dispersion
- Application
    - do not apply for $\Delta W_{eff}/\Delta x < S_{crit}/n$
    - fully apply for $\Delta W_{eff}/\Delta x > nS_{crit}$ [reduce $W_{eff}$, increase x]
    - Linear blending factor else: $f = [S - S_{crit}/n]/[ nS_{crit} - S_{crit}/n]$

For a time-varying release, the method is applied for each individual observer in turn.

The current options are currently implemented in the UDM spreadsheet:

- GSC=1: no correction
- GSC=2, 3, ….9: $S_{crit}=1$, n = GSC
- GSC=10: $S_{crit}=0$: full shape correction between downwind pool edge and start passive
- GSC=11: $S_{crit}=1$,n=1: full correction for $dW_{eff}/dx>1$, no correction for $dW_{eff}/dx<1$

## 11.1 Area source (Kit Fox $CO_2$ experiments)

### 11.1.1 URA continuous experiment KF0712 (F1.75) – detailed analysis

The variations considered are as follows:

- Wind speed $u_a$=1.75 m/s or reduced wind speed $u_a$ = 0.5m/s

- GSC correction:
    - 1 – no correction
    - 2 – n=2, $S_{crit}=1$
    - 10 – $S_{crit}=0$: full on between downwind edge of area source and start passive
    - 11 - $S_{crit}=1$,n=1: full-on for $dW_{eff}/dx>1$, no correction for $dW_{eff}/dx<1$

The correct application of the GSC10 correction has been verified analytically as follows:

- Analytically calculate from un-corrected data [x, $W_{eff}$] the corrected data [$x^{cor}$, $W_{eff}^{cor}$] using equations stated in the theory, and confirmed that analytical values agreed with those obtained from the UDM spreadsheet
- In addition it was confirmed that upwind of passive transition the overall horizontal cloud area is retained following GSC10.

Figure 6 plots the effective cloud half-width $W_{eff}$ versus the downwind distance x from the centre of the ground-level area source. It includes results both before and after GSC, whereby a full correction has been applied during the heavy-gas-regime downwind of the end of the downwind edge (GSC=10). No passive transition occurs for $u_a$ = 0.5m/s, while passive transition occurs for $u_a$ = 1.75 m/s at 40m (prior to correction; 50m after correction). It confirms excellent agreement between the analytically obtained results and those from the UDM spreadsheet.

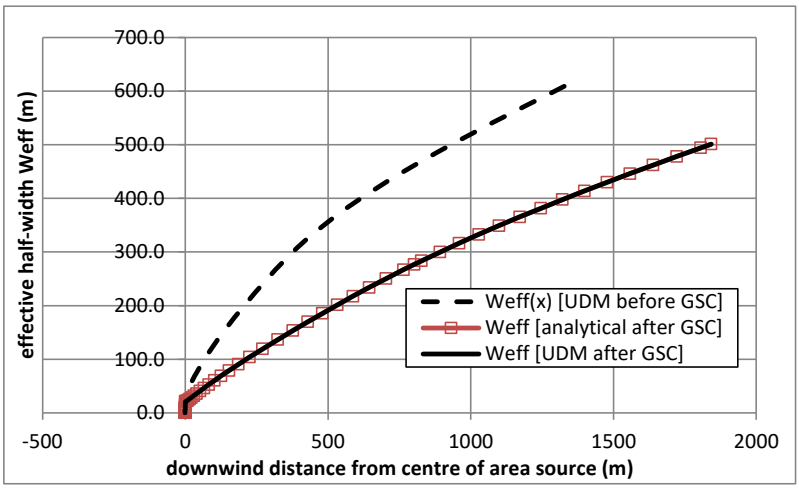


(a) Reduced wind velocity, $u_a$ = 0.5 m/s (heavy only, no passive transition)

(b)

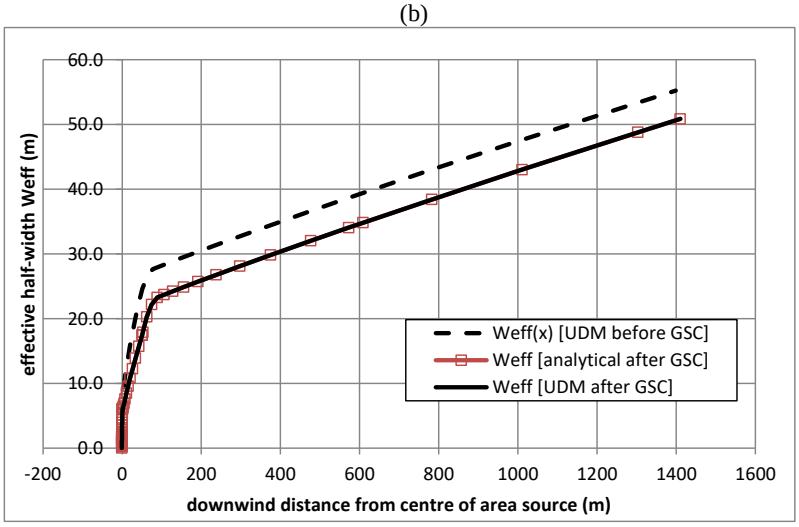


(c) Wind velocity $u_a$ = 1.75 m/s (heavy including transition to passive)

**Figure 6. URA continuous - KF0712; analytical verification of GSC ($W_{eff}$)**

Figure 7 plots UDM results for the range of options for gravity-spreading correction: GSC = 1, 10, 11, 2:

- The full correction (GSC=10) results in a significant reduction of cloud width and increase of concentration for the case of 0.5m/s.
- Immediately downwind of the area source the cloud width is longer than the cloud length.[2]
- Likewise effects of along-wind gravity spreading will be present along the passive transition zone (and gradually reduce) and again this effect has been neglected to avoid added complexity[3]. For $u_a$ = 0.5 m/s no passive transition occurs. For $u_a$ = 1.75 m/s the passive transition zone corresponds to the downwind distance range [40m,78m] prior to GSC and [50m,89m] after GSC.

[2] REFINE. Effects of along-wind gravity spreading will also play a role already along the area source, but these have been neglected to avoid added complexity.

[3] REFINE. Cloud area is NOT conserved downwind of the passive-transition zone. It could be considered to modify the logic along the passive-transition zone such that (a) cloud area would be preserved and (b) and at the downwind edge of the passive transition zone there would be NO effect of GSC (and therefore identical concentrations at a given downwind distance at the downwind edge of the passive transition zone).

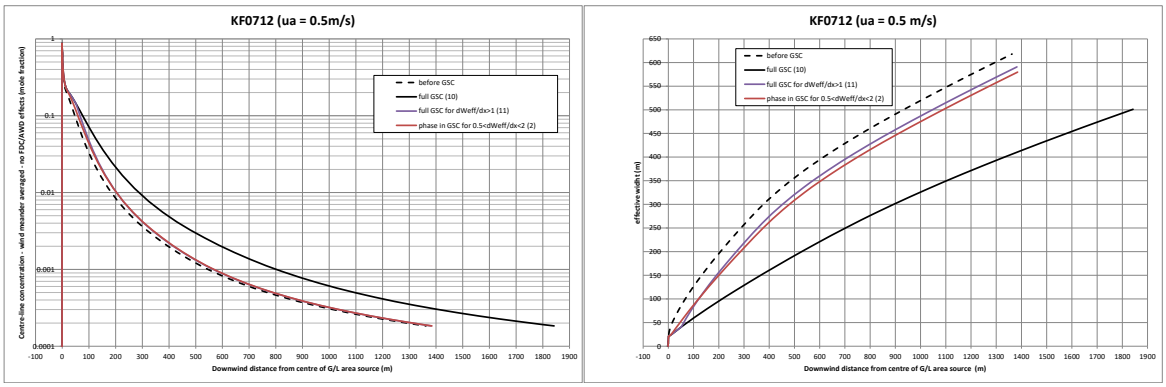


(a) Reduced wind velocity, $u_a$ = 0.5 m/s (heavy only, no passive transition)

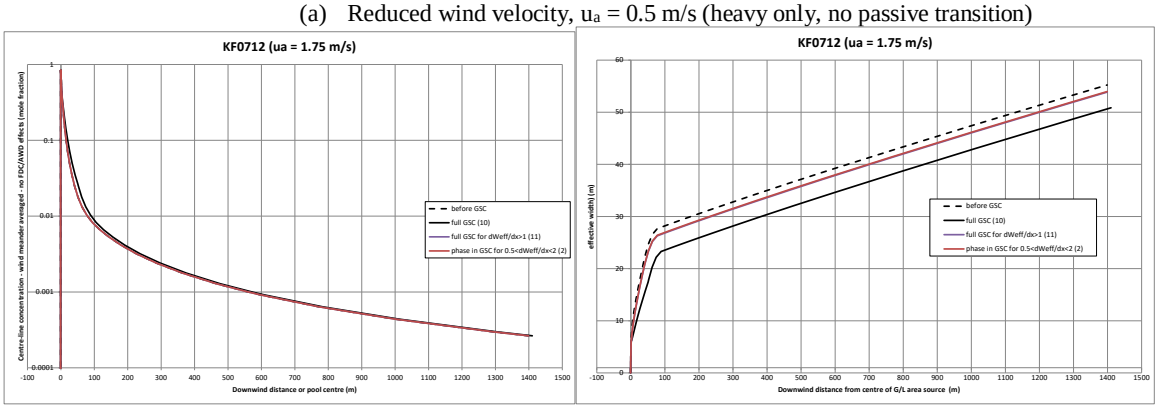


(b) Wind velocity $u_a$ = 1.75 m/s (heavy including transition to passive)

**Figure 7. URA continuous - KF0712; effect of GSC options (concentration and $W_{eff}$)**

## 11.1.2 URA continuous - overall MG, VG results

Table 1 includes overall MG, VG results for all URA continuous experiments for the range of GSC options GSC = 1, 10, 11, 2. It is seen that the full GSC correction (GSC=10) results in an over-prediction of concentrations and under-prediction of the cloud width, and therefore its effect is too strong. Both GSC=11 and GSC=2 options have relatively little overall effect on the predictions, where the recommended GSC=2 option is seen to slightly improve the predictions for the concentrations.

| Data Set | Weather | | S=1 (before GSC) | | | | S=10 (full GSC) | | | | S=11 (full GSC if dWeff/dx>1) | | | | S=2 (phase in GSC for 0.5<dWeff/dx<2) | | | |
|---|---|---|---|---|---|---|---|---|---|---|---|---|---|---|---|---|---|---|
| | Stability class | ua (m/s) | Arcwise conc. | | Width | | Arcwise conc. | | Width | | Arcwise conc. | | Width | | Arcwise conc. | | Width | |
| | | | MG | VG | MG | VG | MG | VG | MG | VG | MG | VG | MG | VG | MG | VG | MG | VG |
| KF0604 | D | 4.09 | 0.92 | 1.21 | 0.87 | 1.03 | 0.82 | 1.32 | 0.99 | 1.01 | 0.92 | 1.21 | 0.87 | 1.03 | 0.922 | 1.212 | 0.874 | 1.026 |
| KF0805 | D | 3.36 | 0.73 | 1.19 | 0.98 | 1.01 | 0.65 | 1.36 | 1.12 | 1.02 | 0.73 | 1.19 | 0.98 | 1.01 | 0.735 | 1.192 | 0.985 | 1.010 |
| KF0702 | E | 4.03 | 0.90 | 1.02 | 1.16 | 1.06 | 0.80 | 1.08 | 1.31 | 1.09 | 0.90 | 1.02 | 1.16 | 1.06 | 0.895 | 1.022 | 1.172 | 1.057 |
| KF0808 | E | 3.36 | 0.62 | 1.29 | 1.06 | 1.02 | 0.54 | 1.51 | 1.21 | 1.04 | 0.62 | 1.29 | 1.06 | 1.02 | 0.618 | 1.293 | 1.068 | 1.017 |
| KF0605 | E | 3.18 | 0.95 | 1.09 | 0.80 | 1.06 | 0.82 | 1.18 | 0.93 | 1.03 | 0.95 | 1.09 | 0.81 | 1.06 | 0.948 | 1.085 | 0.810 | 1.058 |
| KF0703 | E | 2.98 | 0.91 | 1.03 | 1.27 | 1.08 | 0.79 | 1.11 | 1.48 | 1.17 | 0.91 | 1.03 | 1.28 | 1.08 | 0.911 | 1.028 | 1.292 | 1.083 |
| KF0705 | E | 2.82 | 0.94 | 1.02 | 1.15 | 1.03 | 0.81 | 1.10 | 1.38 | 1.12 | 0.94 | 1.02 | 1.17 | 1.03 | 0.944 | 1.022 | 1.173 | 1.036 |
| KF0606 | E | 2.31 | 1.16 | 1.15 | 0.95 | 1.02 | 0.94 | 1.21 | 1.17 | 1.05 | 1.16 | 1.15 | 0.98 | 1.02 | 1.163 | 1.145 | 0.981 | 1.018 |
| KF0811 | E | 2.25 | 1.01 | 1.10 | 0.78 | 1.08 | 0.84 | 1.23 | 0.94 | 1.04 | 1.01 | 1.10 | 0.80 | 1.07 | 1.007 | 1.103 | 0.803 | 1.069 |
| KF0709 | F | 2.24 | 0.95 | 1.01 | 0.87 | 1.04 | 0.78 | 1.09 | 1.08 | 1.04 | 0.95 | 1.01 | 0.91 | 1.03 | 0.947 | 1.011 | 0.899 | 1.034 |
| KF0609 | F | 1.8 | 1.00 | 1.02 | 1.05 | 1.00 | 0.80 | 1.12 | 1.40 | 1.13 | 1.00 | 1.02 | 1.13 | 1.02 | 0.998 | 1.021 | 1.108 | 1.013 |
| KF0712 | F | 1.75 | 1.19 | 1.06 | 1.26 | 1.13 | 0.94 | 1.04 | 1.61 | 1.30 | 1.19 | 1.06 | 1.34 | 1.16 | 1.187 | 1.056 | 1.333 | 1.154 |
| | Average D | 2 | 0.823 | 1.202 | 0.923 | 1.019 | 0.729 | 1.342 | 1.051 | 1.014 | 0.823 | 1.202 | 0.923 | 1.019 | 0.823 | 1.202 | 0.928 | 1.018 |
| | Average E | 7 | 0.913 | 1.096 | 1.005 | 1.049 | 0.783 | 1.195 | 1.180 | 1.075 | 0.913 | 1.096 | 1.018 | 1.048 | 0.913 | 1.096 | 1.023 | 1.048 |
| | Average F | 3 | 1.042 | 1.029 | 1.027 | 1.056 | 0.837 | 1.082 | 1.316 | 1.137 | 1.039 | 1.029 | 1.089 | 1.064 | 1.039 | 1.029 | 1.077 | 1.062 |
| | Average all | 12 | 0.928 | 1.096 | 0.998 | 1.046 | 0.787 | 1.188 | 1.191 | 1.080 | 0.927 | 1.096 | 1.020 | 1.047 | 0.927 | 1.096 | 1.021 | 1.047 |
| | Note | | Original calculations (no FDC or AWD) | | | | Too large effect, too high concentrations | | | | Overall very small effect, close to S=2 | | | | Overall very small effect -> RECOMMEND | | | |

**Table 2. URA continuous; MG, VG values - effect of GSC correction options**

## 11.1.3 URA puff

Figure 8 includes results of effective cloud width and concentration for URA puff experiment KF0714 (F1.4, experiment with smallest measured wind speed). The figure includes the following variations:

- Actual wind speed of 1.4 m/s and reduced wind speed of 0.5 m/s
- GSC = 1, 2 or 10
- Without and with additional time-averaging

It is seen that additional time-averaging has a negligible effect on the results. As for the URA continuous, it is seen that the GSC=10 has a more pronounced effect than GSC=2 and the GSC correction is significantly larger for the lower wind

speed than the larger actual wind speed. For the actual wind speed, the GSC2 correction is seen to have very little effect on the prediction concentration.

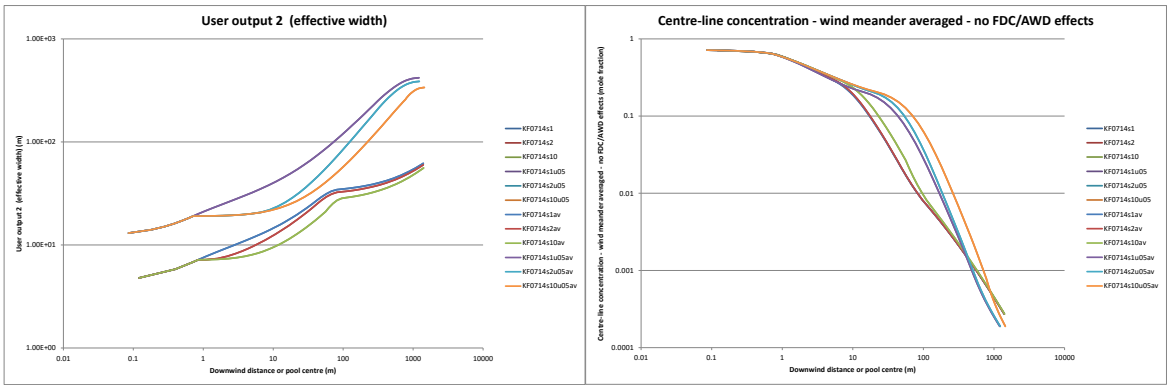


**Figure 8. URA puff KF0714: vary GSC (1,2,10), $u_a$ (1.4,0.5m/s), additional time averaging**

Table 3 includes results for all URA puff experiments. Here alongwind diffusion was applied including additional time averaging, with the Chatwin formula applied to evaluate the along-wind diffusion coefficient $\sigma_x$ in case of stability class D and the Ermak formula applied otherwise. It is seen that using GSC=2 there is very little effect on the MG,VG values (very minor increase in concentrations and very minor decrease in widths, even for stability class F).

| Data Set | Weather | | S=1 (before GSC) | | | | S=2 (phase in GSC for 0.5<dWeff/dx<2) | | | |
|---|---|---|---|---|---|---|---|---|---|---|
| | Stability class | ua (m/s) | Arcwise conc. | | Width | | Arcwise conc. | | Width | |
| | | | MG | VG | MG | VG | MG | VG | MG | VG |
| KF0601 | D | 4.42 | 0.310 | 4.583 | 0.851 | 1.085 | 0.310 | 4.583 | 0.851 | 1.085 |
| KF0801 | D | 4.62 | 0.288 | 4.988 | 1.276 | 1.078 | 0.288 | 4.988 | 1.276 | 1.078 |
| KF0803 | D | 4.31 | 0.399 | 2.411 | 0.850 | 1.049 | 0.399 | 2.411 | 0.852 | 1.048 |
| KF0802 | D | 4.29 | 0.359 | 2.875 | 0.895 | 1.037 | 0.359 | 2.875 | 0.898 | 1.037 |
| KF0804 | D | 4.2 | 0.448 | 1.909 | 0.917 | 1.023 | 0.448 | 1.909 | 0.919 | 1.023 |
| KF0602 | D | 4.03 | 0.343 | 3.297 | 1.065 | 1.033 | 0.343 | 3.297 | 1.068 | 1.033 |
| KF0603 | D | 3.85 | 0.488 | 1.714 | 0.796 | 1.059 | 0.488 | 1.714 | 0.796 | 1.058 |
| KF0806 | D | 3.36 | 0.463 | 1.854 | 0.572 | 1.370 | 0.463 | 1.855 | 0.575 | 1.360 |
| KF0807 | E | 3.24 | 0.597 | 1.307 | 0.606 | 1.321 | 0.596 | 1.308 | 0.612 | 1.306 |
| KF0809 | E | 3.09 | 0.673 | 1.260 | 0.719 | 1.138 | 0.672 | 1.260 | 0.726 | 1.131 |
| KF0706 | E | 2.66 | 0.644 | 1.247 | 0.626 | 1.254 | 0.643 | 1.248 | 0.636 | 1.234 |
| KF0810 | E | 2.47 | 0.519 | 1.657 | 0.721 | 1.140 | 0.519 | 1.660 | 0.736 | 1.125 |
| KF0812 | E | 2.21 | 0.691 | 1.386 | 0.577 | 1.398 | 0.690 | 1.388 | 0.591 | 1.365 |
| KF0704 | F | 2.77 | 0.763 | 1.079 | 0.679 | 1.201 | 0.762 | 1.080 | 0.695 | 1.179 |
| KF0708 | F | 2.61 | 0.790 | 1.155 | 0.686 | 1.169 | 0.789 | 1.157 | 0.704 | 1.148 |
| KF0710 | F | 2.01 | 0.811 | 1.217 | 0.614 | 1.289 | 0.808 | 1.221 | 0.644 | 1.237 |
| KF0607 | F | 1.94 | 0.996 | 1.428 | 0.586 | 1.350 | 0.992 | 1.434 | 0.618 | 1.278 |
| KF0711 | F | 1.93 | 0.822 | 1.221 | 0.610 | 1.298 | 0.819 | 1.225 | 0.641 | 1.242 |
| KF0608 | F | 1.89 | 0.712 | 1.358 | 0.588 | 1.348 | 0.710 | 1.364 | 0.619 | 1.284 |
| KF0714 | F | 1.4 | 0.524 | 1.753 | 0.895 | 1.012 | 0.519 | 1.783 | 1.006 | 1.000 |
| | Average D | | 0.381 | 2.739 | 0.880 | 1.095 | 0.381 | 2.739 | 0.882 | 1.093 |
| | Average E | | 0.622 | 1.364 | 0.647 | 1.246 | 0.621 | 1.365 | 0.658 | 1.229 |
| | Average F | | 0.762 | 1.301 | 0.635 | 1.262 | 0.759 | 1.307 | 0.664 | 1.217 |
| | Average all | | 0.549 | 1.773 | 0.719 | 1.194 | 0.548 | 1.777 | 0.735 | 1.173 |
| | Note | | Original calculations (AWD&time aver.) | | | | Overall very small effect -> RECOMMEND | | | |

**Table 3. URA puff; MG, VG values - effect of GSC2 correction**

## 11.2 Elevated horizontal 600s fixed-duration release (flashing-liquid $Cl_2$)

The issue of absence of downwind gravity spreading (i.e. presence of too wide clouds) in conjunction with low wind speed is most paramount for many 10 minute Safeti-NL release scenarios with weather F1.5 (horizontal release at 1 m height).

This section considers the example case of a vessel filled with saturated chlorine liquid at 8.85°C (inventory of 25 $m^3$, liquid total height of 3 meter, bottom of vessel at 1m height, hole at bottom of vessel, horizontal release).

Two cases were analysed in detail, i.e.

- the case with a reduced droplet size of SMD=100µm such that no rainout occurs (no pool observers)
- the actual calculated case with SMD=247µm involving rainout (including pool observers).

## 11.2.1 Reduced droplet size 100µm without rainout

Using separate spreadsheet calculations, Figure 9 verifies analytically the correct application in the UDM of the gravity spreading correction (GSC=10), where significantly reduced spreading is seen following transition to passive dispersion (at uncorrected distance of 451m and corrected distance of 790m).

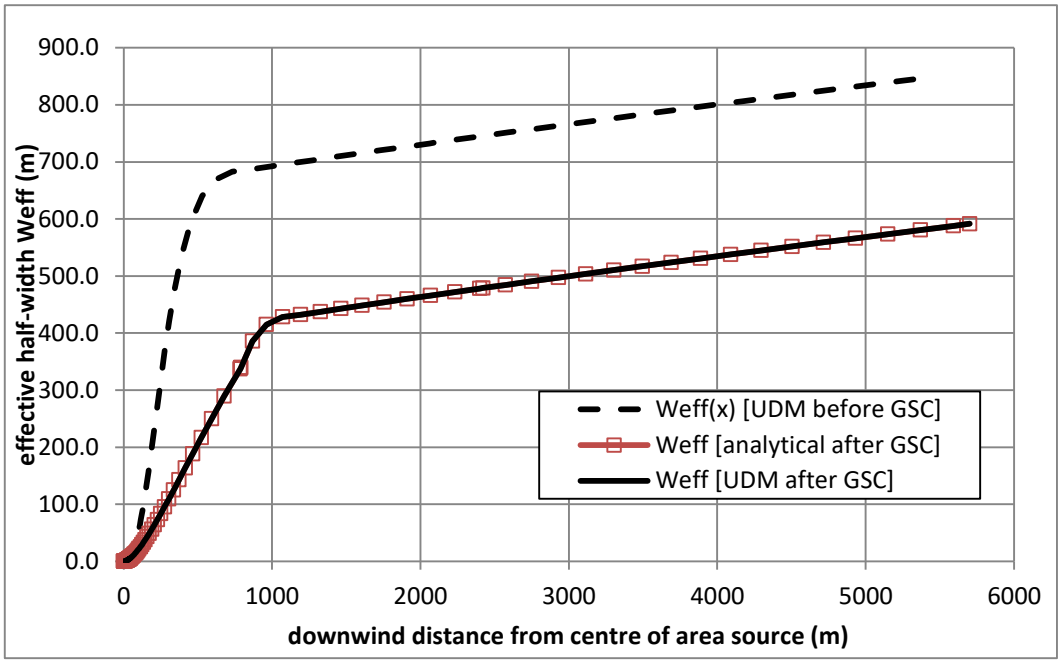


**Figure 9. $Cl_2$ 600s release (SMD=100µm); analytical verification of GSC=10 ($W_{eff}$)**

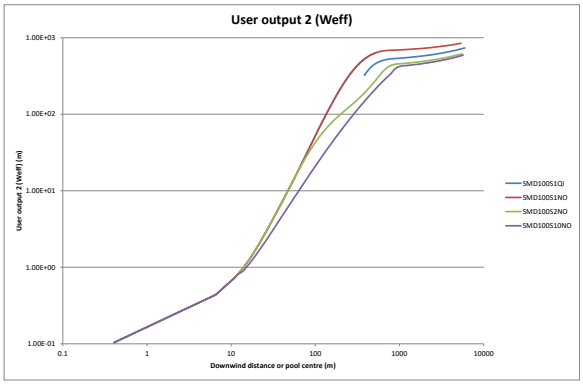


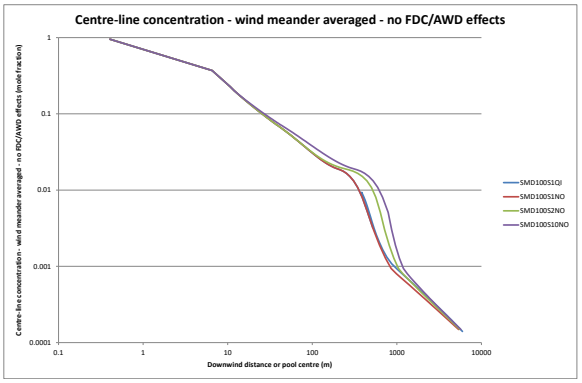

**(a)** Effective width (b) C/L concentration (before AWD)

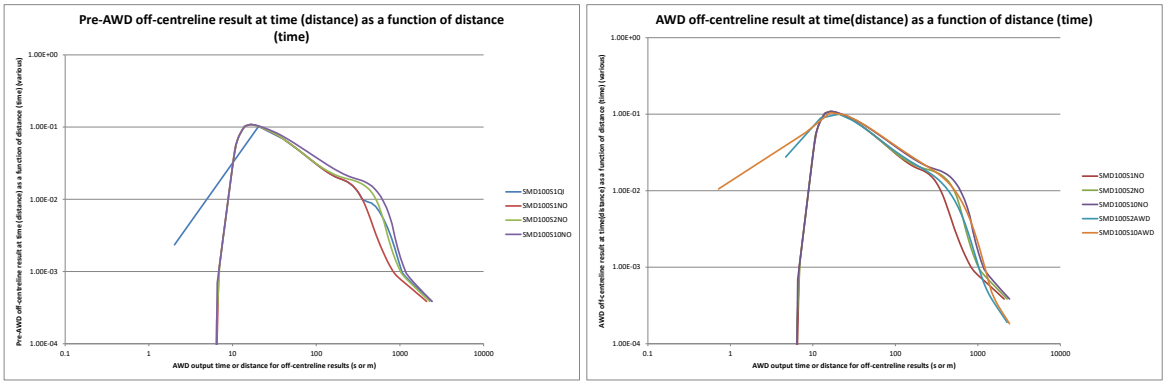


**(c)** G/L concentration (pre-AWD) (d) G/L concentration (post-AWD)

**Figure 10. $Cl_2$ 600s release (SMD=100µm); GSC= 1,2 or 10; QI, no AWD or AWD**

Figure 10 includes results of UDM spreadsheet run**s** using the following variations:

- Method for modelling of along-wind-diffusion effects: QI, no AWD, AWD
- Method of GSC: 1 (none), 2(default), 10 (full on)

The upper two plots below plot the effective half-width $W_{eff}$ and the C/L concentration (before AWD effects) and they demonstrate the effect of GSC (reducing cloud width and increasing cloud length) with increased effects for GSC=10. The lower two plots plot the ground-level concentration (maximum value over all time) before and after AWD. It demonstrates the effect of increasing the concentration because of GSC, and the effect of concentration reduction because of AWD. Figure 10d indicates that the post-AWD 8.0 G/L concentration is larger than the QI concentration.

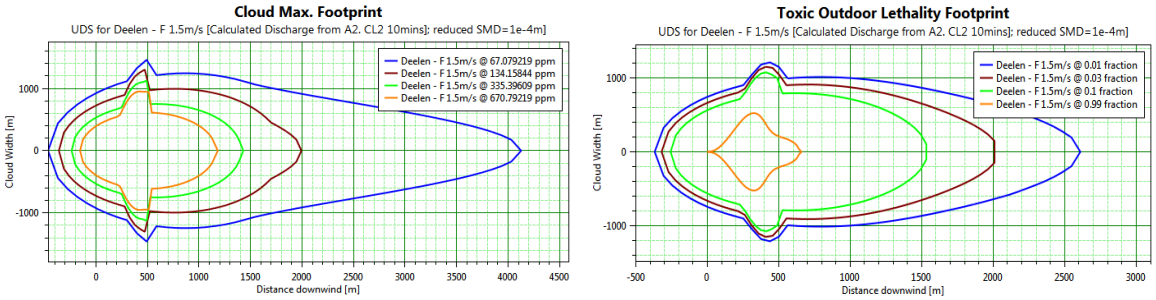


**Figure 11. $Cl_2$ 600s release (SMD=100µm); Safeti-NL predictions (QI, no GSC)**

Figure 11 depicts results for maximum concentration and lethality using the old QI method, where a transition from the continuous cloud to the instantaneous cloud was made at distance 518m.

Figure 12 shows maximum concentration and lethality contours (Safeti-NL 8.0 GUI) before (left plot) and after (right plot) GSC=2 or GSC=1- correction, with the QI ratio of cloud width to cloud length increased to its maximum value of 10 such that QI does NOT occur (i.e. results before AWD). The figure demonstrates the reduction of the width and the lengthening of the cloud due to the downwind gravity spreading correction. Thus this results in more conservative predictions. The concentrations from the above Safeti-NL run were confirmed to be close to that of the UDM spreadsheet run. The passive transition was shown to take place at 451m. The figure shows that downwind of 451m the cloud length is larger than the cloud width, and therefore the GSC may need refinement along the passive transition zone.

Figure 15 includes results after GSC=2 correction and after AWD. For the 600s release (wind speed 1.5 m/s) one would expect effects of AWD to be small for distances less than 600*1.5=900m and this is confirmed by comparing Figure 15 and Figure 12b.

By comparing Figure 11 and Figure 12 one can compare the results for maximum concentrations and toxic lethality for the old and new methods. Note that the QI transition results in unrealistic lethality upwind of the release point. It also shows that the QI downwind distance to the 1% lethality is smaller. Thus in case of no rainout and the presence of a QI transition, the old QI method may result in reduced lethality compared to the new method.

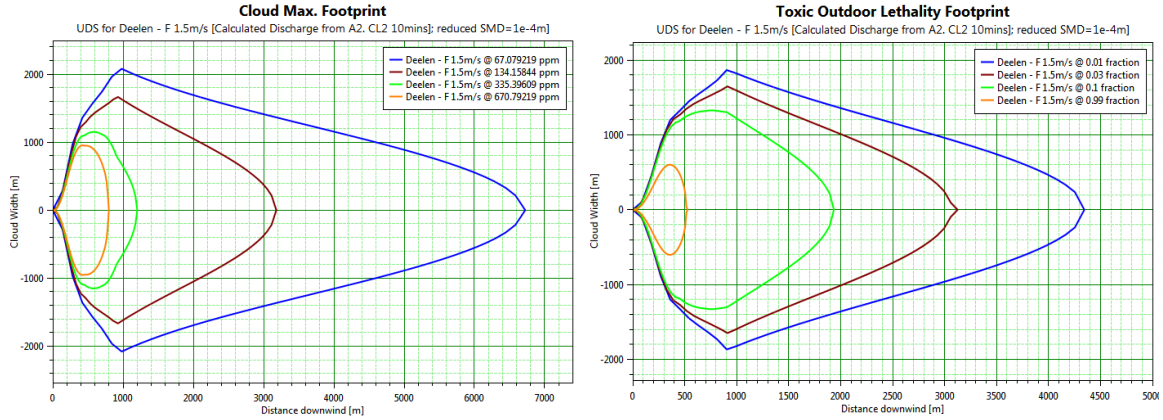


(a) Before GSC

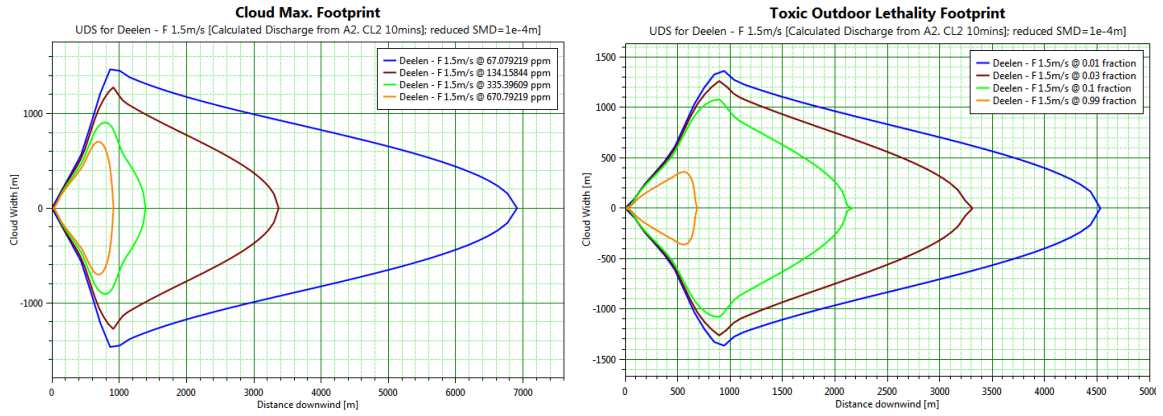


(b) After GSC=2

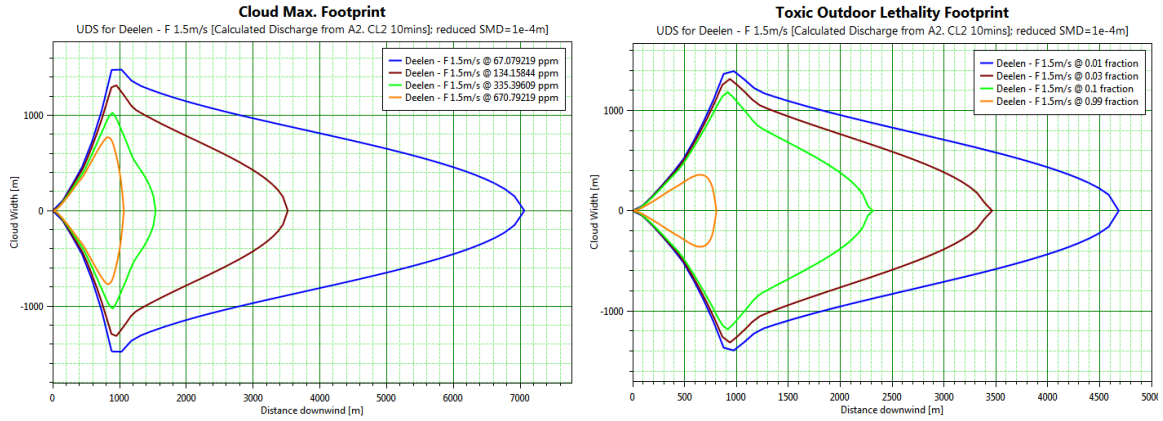


(c) After GSC=10 (full GSC)

**Figure 12. $Cl_2$ 600s release (SMD=100µm); Safeti-NL predictions (GSC=1,2,10; no AWD)**

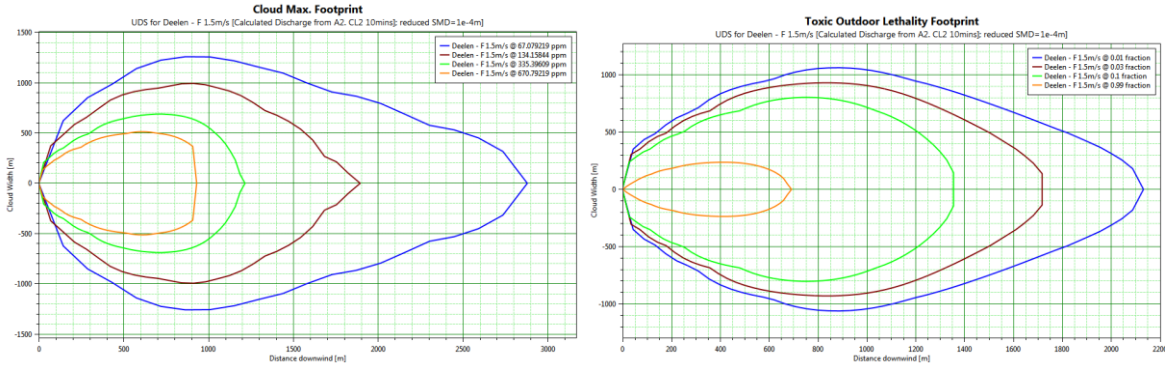


**Figure 13. $Cl_2$ 600s release (SMD=100µm); Safeti-NL predictions (GSC=2 with AWD)**

## 11.2.2 Actual droplet size 247µm with rainout

Secondly results are presented with the calculated droplet size.

Observer trajectories

As shown in Figure 14, 50 % rainout occurs at 22m downwind with a maximum pool radius of 11m. Thus the furthest upwind edge of the pool is at x=11m, i.e. downwind at the release. A release observer is released at 0m. An additional 9 pool observers are subsequently at the end of 9 equal pool-mass intervals, where the first 4 pool observers are released before the end of the release. In addition observers are released at the end of the release (600s), and shortly after the end of the release to mark the start of the trailing cloud. Thus a total number of 12 observers is released. I do not fully understand the release time of the first trailing observer – see spreadsheet (sheet SMD247OMCAWD; and also see plot plot).

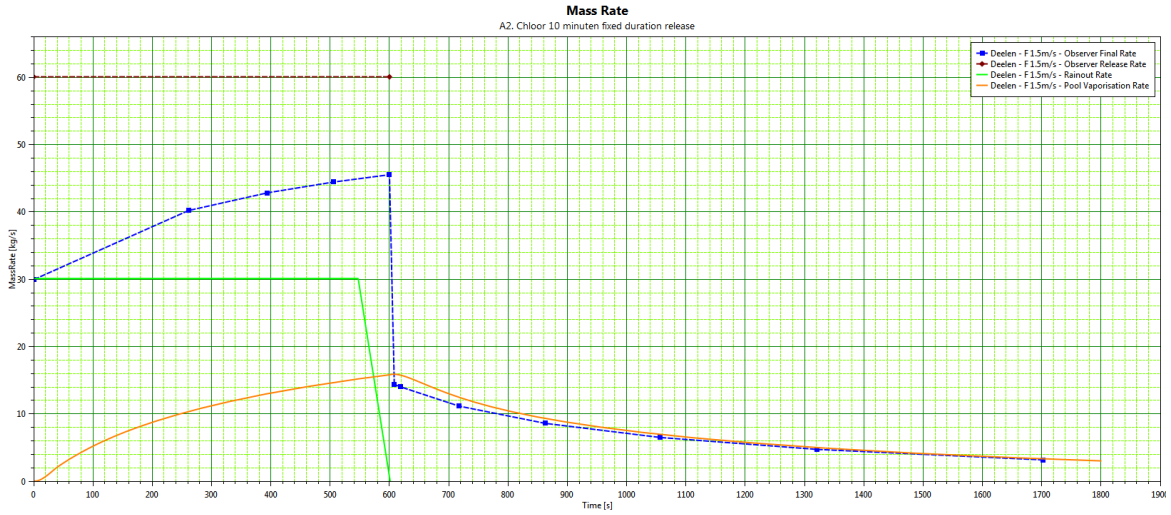


**Figure 14. $Cl_2$ 600s release (SMD=247µm); release rate, rainout rate, pool evaporation rate, and observer mass rates**

Figure 15 depicts the movement of the observers as function of time. It indicates the above observer release times. It indicates that GSC2 correction is very small, while the GSC10 correction is much more substantial. Note that no time-shifting was carried out, and therefore the OMC correction does not affect the observer locations.

Figure 16 includes UDM results.

- Figure 16a (observer effective width) shows that the GSC correction is only applied downwind of the downwind edge of the pool (x=42.3m), and it confirms that the GSC2 correction is less strong that the GSC10 correction (less reduction of the cloud width and less lengthening of the cloud).
- Figure 16b (pre-AWD observer centre-line concentration) shows the sharp drop of the concentration at the point of rainout (at downwind distance x=21m). It is seen that for some of the observers the OMC correction result in a significant drop in the concentrations. This may be for the two subsequent observers who are released at the end of the spill and shortly after the spill. The trailing observer would be released with a significant lower speed, and this would result in a significant reduction of both concentrations.
- Figure 16c shows the pre-AWD maximum concentration over all times. It shows the effect of the GSC correction (increased concentrations), and a minor effect of the OMC correction in the near-field (reduced concentrations). Note that the effect of the rainout is no longer visible, since the maximum concentration at the rainout point is dominated by the trailing pool observers.
- Figure 16d shows the AWD maximum concentration over all times. It shows the effect of the GSC correction (increased concentrations), and a minor effect of the OMC correction in the near-field (reduced concentrations). This shows the AWD reduction of the concentration in the far field. The 7.2 predictions for the maximum concentration would be expected to be closest to those predicted for SMD247S1; 8.0 predictions may be larger because of GSC effects, while they may be smaller (particularly in the far-field) because of AWD effects.

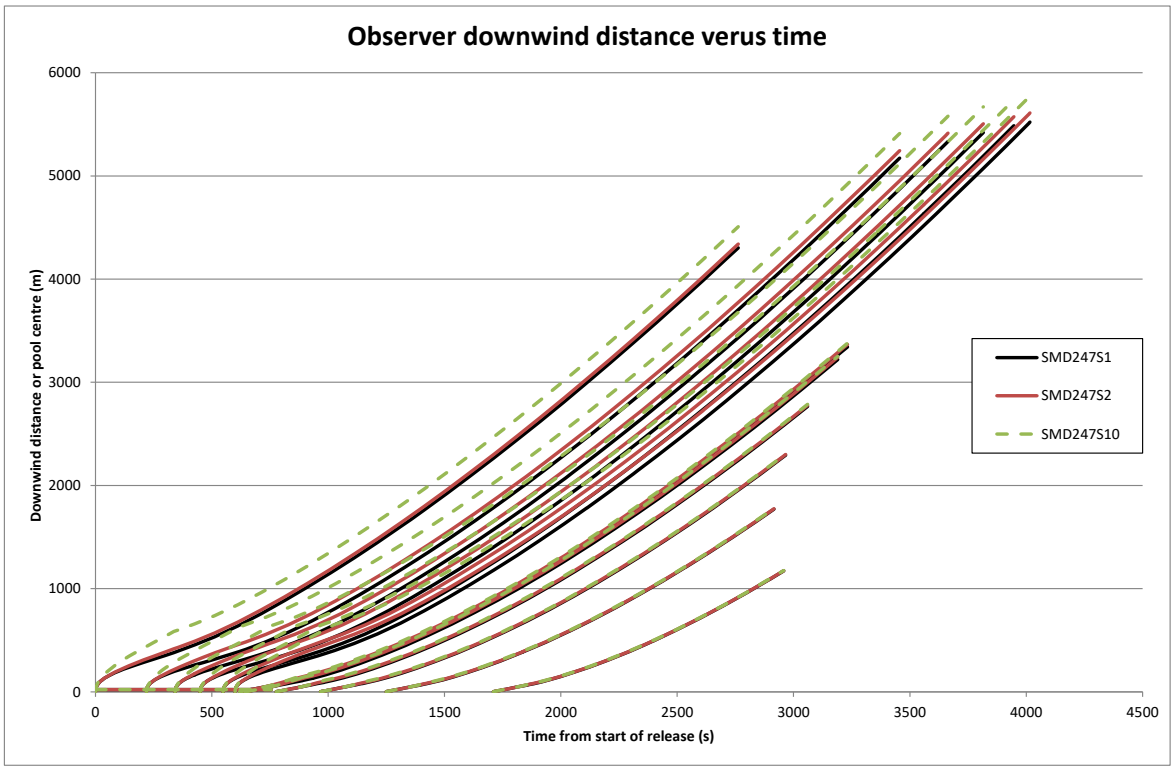


**Figure 15.** **$Cl_2$ 600s release (SMD=247µm); release and pool observer trajectories**

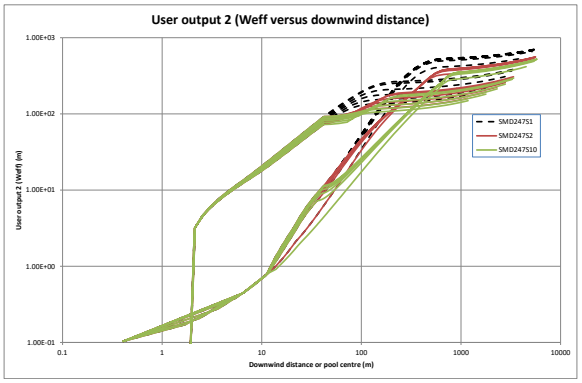


**(a)** Effective width

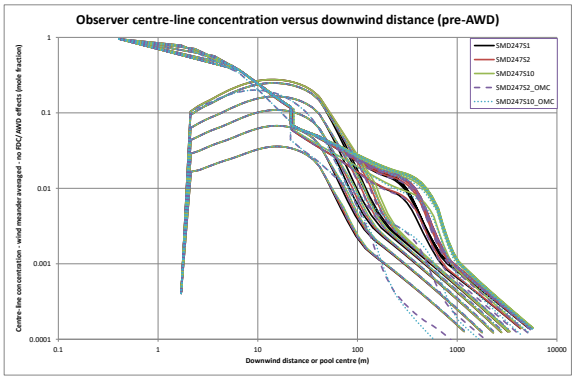


(b) C/L concentration (before AWD)

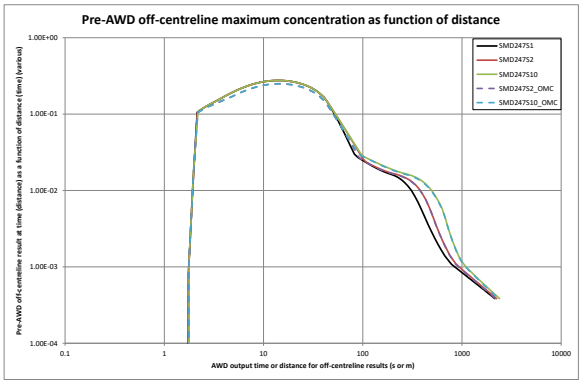


(c) G/L concentration (pre-AWD)

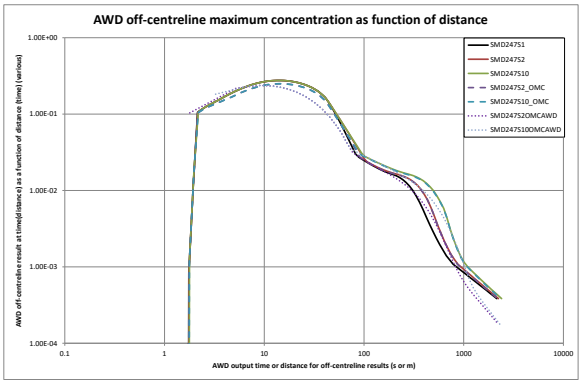


(d) G/L concentration (post-AWD)

**Figure 16.** **$Cl_2$ 600s release (SMD=247µm); GSC= 1, 2 or 10 (without or with AWD)**

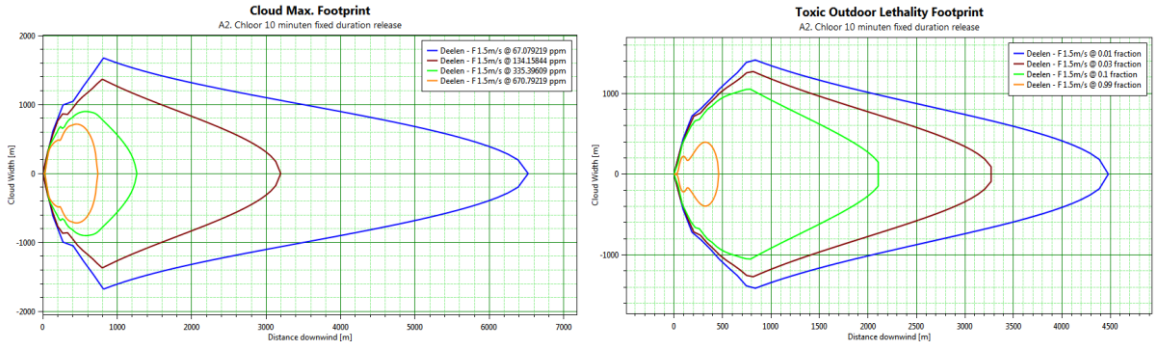


(a) before GSC and OMC

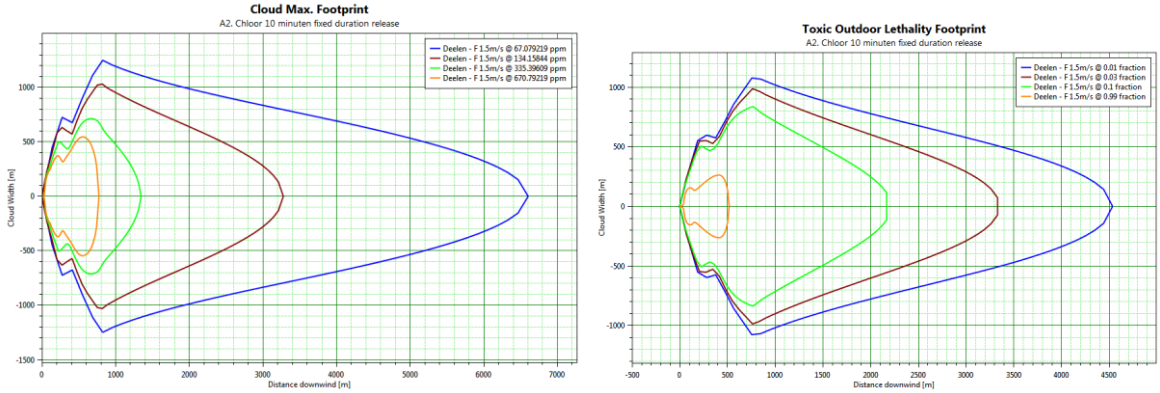


(b) after GSC2 and before OMC

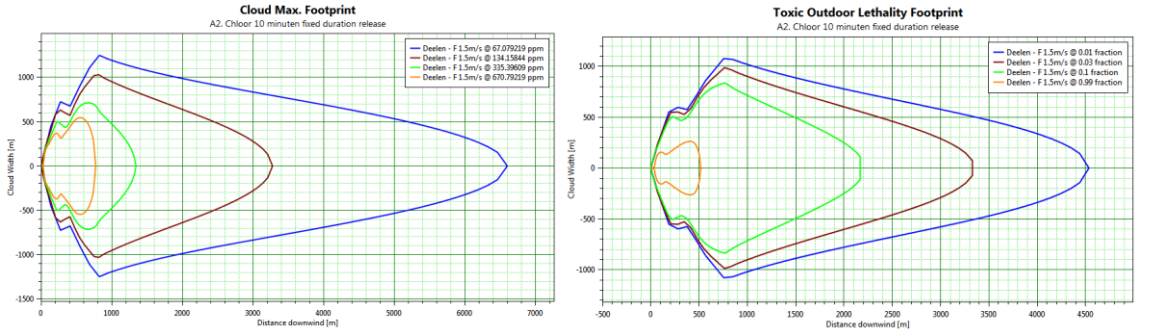


(c) after GSC2 and OMC (footprint at 0m height); pre-AWD [almost identical!!]

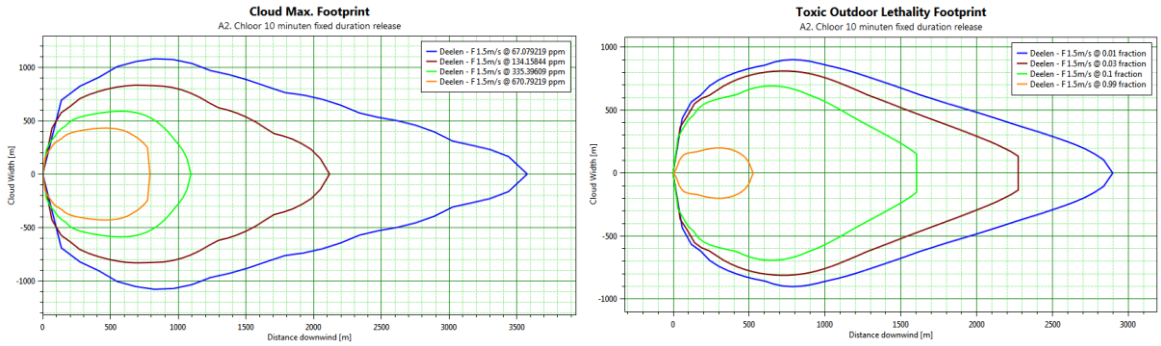


(d) after GSC, OMC (footprint at 1m height); post-AWD

**Figure 17. $Cl_2$ 600s release (SMD=247µm); Safeti-NL predictions (GSC=1 or 2; no AWD)**

Figure 17 plots results before and after GSC for maximum concentrations and lethality footprints. It is seen that e.g. at 500m the toxic footprint width is still larger after GSC than 500m, because GSC=2 applies a partial correction only. GSC=10 would have resulted in better behaviour. The effects of OMC are very small.

## About DNV

We are the independent expert in risk management and quality assurance. Driven by our purpose, to safeguard life, property and the environment, we empower our customers and their stakeholders with facts and reliable insights so that critical decisions can be made with confidence. As a trusted voice for many of the world's most successful organizations, we use our knowledge to advance safety and performance, set industry benchmarks, and inspire and invent solutions to tackle global transformations.

## Digital Solutions

DNV is a world-leading provider of digital solutions and software applications with focus on the energy, maritime and healthcare markets. Our solutions are used worldwide to manage risk and performance for wind turbines, electric grids, pipelines, processing plants, offshore structures, ships, and more. Supported by our domain knowledge and Veracity assurance platform, we enable companies to digitize and manage business critical activities in a sustainable, cost-efficient, safe and secure way.

DNV | digital@dnv.com | dnv.com/digital

## REFERENCES

[i] Ermak, D.L., 1986. Unpublished notes on downwind spreading formulation in finite-duration release version of SLAB, Lawrence Livermore National Laboratory, California